ENGINEERING RESEARCH INSTITUTE
UNIVERSITY OF MICHIGAN
ANN ARBOR

A STUDY OF THE PREPARATION OF NICKEL-ZINC FERRITES

Technical Report No. 58
Electronic Defense Group
Department of Electrical Engineering

By: C. F. Jefferson
D. M. Grimes

Approved by: H. W. Welch, Jr.

Project 2262

TASK ORDER NO. EDG-6
CONTRACT NO. DA-36-039 sc-63203
SIGNAL CORPS, DEPARTMENT OF THE ARMY
DEPARTMENT OF ARMY PROJECT NO. 3-99-04-042
SIGNAL CORPS PROJECT NO. 194B

January, 1956

TABLE OF CONTENTS

LIST OF ILLUSTRATIONS

LIST OF ILLUSTRATIONS (Cont'd.)

LIST OF TABLES

ABSTRACT

The solid state reaction involved in the formation of ferrites is discussed. The manufacturing processes are viewed in terms of their contributions to this reaction. Data on the formation of ferrous iron in stoichiometric ferrites as well as in ferrites containing excess iron is given, along with some magnetic measurements of the material.

A STUDY OF THE PREPARATION OF NICKEL-ZINC FERRITES

1. STATEMENT OF THE PROBLEM AND CONCLUSIONS

1.1 Statement of the Problem

The preparation of magnetic ferrite cores suitable for use in electrical circuits requires special precautions during the manufacturing process. An attempt to reproduce cores with the same magnetic properties in successive preparations, even when seemingly the greatest detail is followed in the procedure, often results in failure. This can only mean that the magnetic properties of the final product are sensitive to the slightest variation in the manufacturing procedure. This report considers the relative importance of some of the more obvious parameters.

One of the major reasons for the difficulty in repeating detailed magnetic properties in different ferrites is that the spinel structure is relatively complex with many opportunities for the metallic ions or cations to occupy improper lattice positions. There are two different types of lattice sites available for the cations, customarily designated as A and B sites. In the perfect spinel lattice the unit cell consists of 8 MFe_2O_4 where M designates the particular divalent cation added. In any unit cell there are 64 A sites and 32 B sites, of these 8 A sites and 16 B sites or 1/8 of the A and 1/2 of the B are occupied by metallic ions or cations. For a perfect lattice only those sites with cubic symmetry can be occupied.

One fourth of a unit cell is illustrated in Figure 1, where the sites are designated by the letters. Note that the A sites are surrounded by four oxygens forming a tetrahedron, while the B sites are surrounded by six oxygens forming an octahedron. Now it is not enough that just the precise sites corres-

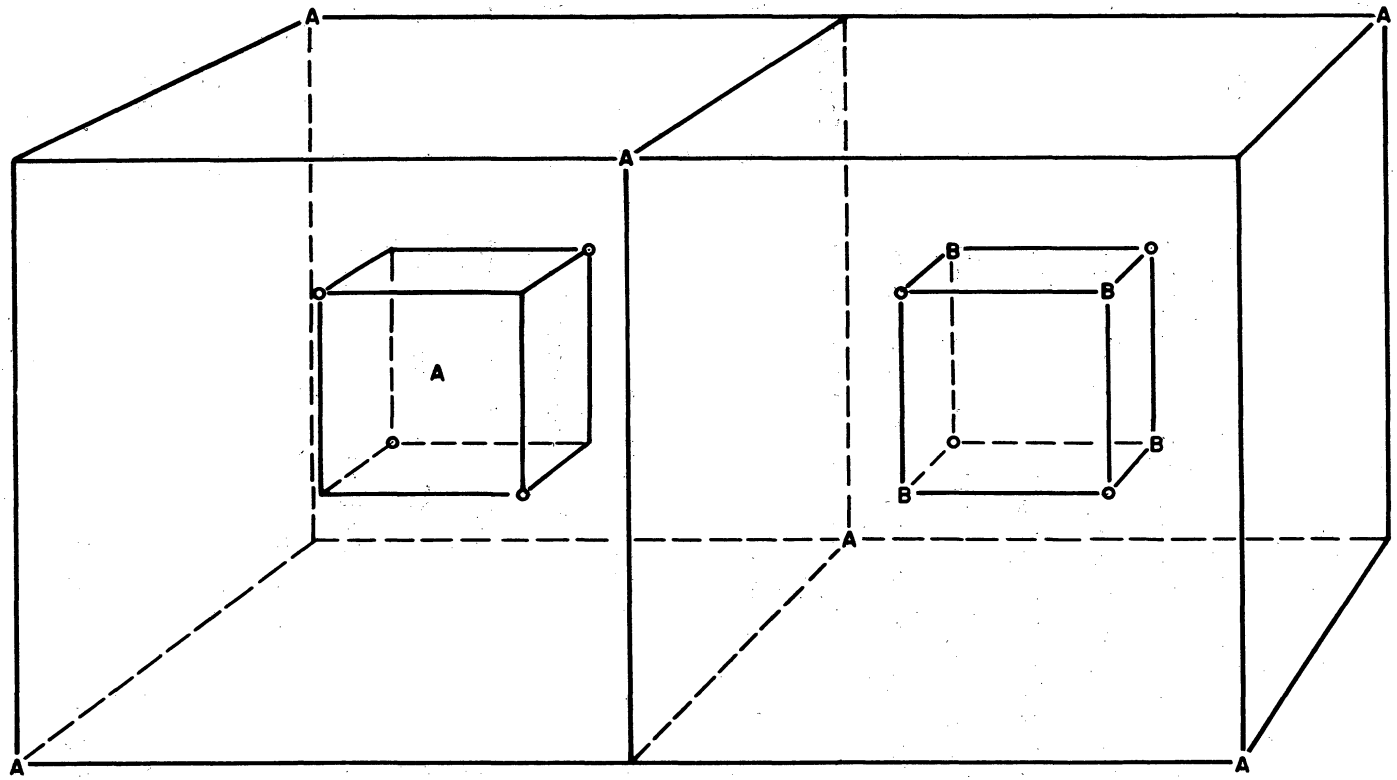

SYMBOL	NORMAL STRUCTURE		INVERSE STRUCTURE	COORDINATE NUMBER
	$MgAl_2O_4$	MFe_2O_4	MFe_2O_4	
A	$1\ Mg^{++}$	$1\ M^{++}$	$1\ Fe^{+++}$	4 (TETRAHEDRAL SITES)
B	$2\ Al^{+++}$	$2\ Fe^{+++}$	$1\ M^{++},\ 1\ Fe^{+++}$	6 (OCTAHEDRAL SITES)
o	$4\ O^{--}$	$4\ O^{--}$	$4\ O^{--}$	OXYGEN

FIG. 1
THE SPINEL STRUCTURE

ponding with cubic symmetry be occupied but it is also required that the cations be on the proper sublattice. It has been found experimentally that certain cations show a preference for a particular type of lattice site, for example when mixed with Fe_2O_3 it is found that Ni cations prefer the B sites while Zn cations prefer the A sites. Ferrous iron like Ni prefers the B sites. In addition to just the proper lattice sites being occupied by the cations, the cations must occupy the proper sublattice sites and only these sites. Further we must insist that they be distributed throughout the material uniformly, that is, there must either be an ordered arrangement of each specific cation on its choice of sublattices or it must be distributed purely at random. Restating, we must insist in a mixed ferrite Ni and Zn that we not have regions of nickel ferrite and regions of zinc ferrite but a homogeneous material! These complexities are over and above the complexities customarily present in the case of the ferromagnetic metals with their relatively simple structure.

Turning from the atomistic scale up many orders of magnitude dimensionally to the microscopic scale to consider the granular nature of the material, such questions as the effect of granular imperfections or second phases upon magnetic phenomena and the effect of grain size upon magnetic properties must be considered. Fortunately, all imperfections do not have to be removed and all grains need not be of the same size, but the material must be macroscopically homogeneous. Thus the imperfections present must be scattered uniformly throughout the material and must be repeatable from batch to batch. Likewise the grains, although not necessarily all the same size, must be distributed according to some repeatable function.

It has been experimentally determined that those ferrites for which the divalent cations prefer the B sites (inverted spinels) are ferrimagnetic and those for which the divalent cations prefer the A sites (normal spinels) are not ferri-

magnetic. Further, a ferrite with some divalent cations on the A sublattice and some on the B sublattice carries a larger spontaneous moment than a ferrite with cations on the B sublattice only. Therefore, to obtain large values of susceptibility it is necessary to mix the two types of ferrites. Such a ferrite is a mixed nickel zinc ferrite.

The magnetic properties of ferrites initially became of importance because of the combination properties of high magnetic permeability together with an electrical resistivity many order of magnitude higher than that of the metals. Based upon calculated eddy current losses alone, the advent of these materials promised the availability of electronically useable ferromagnets well up into the hundreds of megacycles. It was soon discovered that secondary losses masked in metals by the eddy currents became important and limited the usage of such materials.

The extra loss term was accounted for phenomenologically by Landau and Lifschitz[1], but the physical source of this damping factor is not understood. However, it is presumably due to some sort of coupling between magnetic and elastic fields (spin-lattice coupling). One mechanism would be ionic motion. Ionic motion would include the moving of ions from a point of high magnetic energy concentration to one of lower energy concentration. These ions could be either interstitially located or they could be on the correct lattice sites. Another mechanism would be electron transfer between nearest neighbor cations which, because of the electron spin, would result in different local energy concentrations.

It has long been considered that the conductivity of magnetite[2] was probably due to electronic transfer from a Fe^{2+} to a Fe^{3+} cation. It was indicated by Wijn and van der Heide[3] that this mechanism was also responsible for

the low frequency magnetic losses. Later Smit[4] showed that the activation energy controlling the conductivity was the same as that controlling the low frequency losses. Recently Galt[5] has calculated an effective damping coefficient due to this relaxation and its resulting effect upon the anisotropy.

Other factors, currently unexplained, also enter. What is the loss mechanism in the absence of ferrous iron? What role is played by magnetostrictive coupling effects? Due to a relatively large positive magnetostrictive constant λ_{111} in magnetite, the polycrystaling magnetostriction $\bar{\lambda}$ is positive. For polycrystalline nickel ferrite $\bar{\lambda}$ is negative. Just what role $\bar{\lambda}$ plays in determining the total loss is not known, but according to Harvey, Hegyi and Leverenz[6] a nickel-iron-zinc ferrite fired at 1400° C in air undergoes a zero magnetostriction at about 56 mole% Fe_2O_3. There can thus be little question but that the presence of ferrous iron plays an important role in the determination of the magnetic losses.

It is apparent that in order to reproduce both the susceptibility and the phase angle of the internal magnetization, phenomena on two different orders of magnitude of dimensions must be controlled. First the proper cations must be located on the proper lattice and sublattice sites with the proper homogeneity. Second, the grains must be uniform in composition or at least if a second phase is present the phases must be well mixed and the distribution of grain sizes must be repeatable.

In section 2.1 of this report the solid state reaction is considered. The manufacturing process, viewed in terms of the solid state reaction is discussed in section 2.2. In section 3, non-stoichiometric ferrites are discussed. The main topics are the formation of ferrous iron and the related magnetic behaviour.

The conclusions derived from the work discussed in Sections 2 and 3 are presented in the next paragraph. There are still many unknown factors in the solid state reaction so that the work cannot be considered to be complete. Some of these factors are suggested for further study.

1.2 Conclusions

The processes involved in the formation of a ferrite from the component oxides consist of the reaction between the oxides to form the spinel structure, the densification of the material, diffusion of the cations to form a homogeneous mass, and grain growth. The method of preparation of the material influences the rate and temperature at which the various changes occur. The temperature at which the spinel formation is complete, as measured by the disappearance of the oxide lines in the X-ray diffraction pattern, can be reduced considerably by coprecipitation of the material. The densification rate can be influenced by the compactness of the green core. The part played by diffusion in obtaining a homogeneous core is determined by the extent of mixing. Grain growth is continuous throughout all of the times and temperatures investigated. A more thorough investigation of grain growth and its influences on the magnetic properties is in progress and will be reported later as will a detailed study of fluxing agents.

The magnetic properties of the core appear to be determined by a summation of the various changes in the physical and chemical properties. While the formation of the spinel structure is necessary for the development of the magnetic properties, it is not enough in itself. An understanding of other changes in the material is necessary in order to interpret the magnetic properties. The distribution of the cations by diffusion, as measured by the ferrous iron con-

tent and the Curie temperature, appears to occur fairly early at 1210°C. The Curie temperature appears to have reached a constant value before the magnetic permeability has ceased changing. Figure 2 is a plot of μ_1 as a function of temperature showing the progression of the various changes. There is an overlapping of the processes so it is difficult to attribute the change in magnetic properties to any one process.

The formation of ferrous iron occurs at temperatures below about 1300°C in the initial stages of sintering and disappears on further sintering. This has been interpreted in terms of a non-stoichiometric distribution of the oxides. At higher temperatures the ferrous iron appears to be due to decomposition of the ferrite.

The formation of ferrous iron in non-stoichiometric cores appears to be determined by the solubility of Fe_3O_4 in the Ni-Zn ferrite in the two phase area, and approach the theoretical limit in the one phase area. This point has not been clarified, and work is being continued on it.

As the amount of excess Fe_2O_3 is increased, the magnetic permeability decreases and the Q increases. The extent of oxidation on cooling appears to affect the Q, but neither μ_1 nor the Curie temperature. The fact that the Curie temperature does not change is somewhat surprising, and not understood at present.

Annealing of a porous core at 800°C oxidizes the ferrous iron and decreases μ_1 and Q. Annealing a dense core at the same temperature increases the Q and does not affect the magnetic permeability.

Much of the explanation of the behavior of non-stoichiometric material appears to lie in understanding the phase diagram of the system. This is left for future study.

THE INFLUENCE OF SINTERING TEMPERATURE
ON THE SOLID STATE REACTION
FIRING TIME, 4 HOURS
[Ni.4 Zn.6 Fe2 O4]
FERROUS IRON FORMATION
GRAIN GROWTH
DENSIFICATION
SPINEL FORMATION
REAL PERMEABILITY
TEMPERATURE (°C)
0
100
200
300
400
500
600
700
800
900
1000
1100
1200
0
200
400
600
800
1000
1200
1400
1600

FIG 2

2. THE PREPARATION OF NICKEL-ZINC FERRITES

2.1 The Solid State Reaction

2.1.1 Reaction between the oxides to form the spinel structure.

Before firing, neighboring oxide particles are often the oxides of different metals. As the thermal energy of the material increases at some point it becomes large enough so some cations are loosened from the lattice sites. Once a cation is loosened it takes but relatively little energy for it to move through a lattice. The result is that at least one cation diffuses into the oxide lattice of the other metal. When a sufficient number of foreign cations are thus arrayed the spinel structure forms. The ordering is initially relatively low and the spinel x-ray diffraction lines are broad.

Using x-ray methods, Kedesdy and Katz[7] found that the spinel structure starts to form at 600°C for $ZnFe_2O_4$ and 700°C for $NiFe_2O_4$, with temperatures for spinel formation of mixed NiO and ZnO ferrites intermediate between these two temperatures. Guillissen and Rysselberghe[8] found by chemical analyses of unreacted Zn in a mixture of ZnO and Fe_2O_3 that reaction to form the ferrite started slightly below 600°C. In this case the extent of reaction reached an equilibrium value after several hours, such that to further the reaction the temperature had to be increased. Hopkins[9] found that the reaction rate was influenced by the temperature of preparation of the Fe_2O_3. It was found that Fe_2O_3 was transformed into a less reactive form at 675°C. Activation energies for the formation of $ZnFe_2O_4$ from the two forms of Fe_2O_3 were found to be 110 K cal/mole for the high temperature form of Fe_2O_3 and 57 K cal/mole for the low temperature form.

Okamura and Simorzaka[10] investigated the rate of formation of $NiFe_2O_4$

with respect to the method of mixing. They concluded that with mechanical mixing diffusion was the rate-controlling step, while with coprecipitated material diffusion was not so important. The activation energy of mechanically mixed oxides was found to be 44 K cal/mole, for the coprecipitated oxides it was found to be 25 K cal/mole. They found no correlation with the appearance of the spinel structure in the x-ray diagrams and the magnetic intensity of the sample, from which they concluded that there was a non-magnetic and a magnetic spinel structure. C. Wagner suggests the rate-controlling mechanism to be the diffusion of the components through a layer of ferrite formed at the interface of the two reacting oxides. Yost[11] states that this mechanism can be used to explain the formation of spinels and silicates. Linder[12], using radio tracers, found that the Wagner theory explained the reaction rates of silicates and of ZnO and Fe_2O_3 to form the spinel $ZnFe_2O_4$. This type of mechanism explained the rate of formation of $NiFe_2O_4$ in the mechanically mixed material prepared by Okamura and Simorzaka.

We have observed in this laboratory that the spinel structure forms within 3 minutes at 1210°C such that no oxide lines remain in an x-ray diffraction diagram. The low frequency permeability, however, increases with the time at temperature up to 900 minutes at 1210°C. The oxide diffraction lines in coprecipitated material have disappeared in four hours at 350°C, yet the magnetic permeability is very low. It therefore appears that evidence of reasonably complete spinel structure formation is not sufficient evidence for the completion of the final magnetic properties of the ferrite. There is some evidence to indicate that spinel line sharpness is more closely related to the magnetic properties. However, other changes must be considered in order to understand the processes involved in the total reaction.

2.1.2 The Densification Process. The densification process here considered is not concerned with the x-ray density of the material but with the apparent density of the bulk material. The change in apparent density is simply a measure of the change of porosity of the material. In order for material to densify, it is necessary that some process or processes involving material transport occur. The driving force for this movement is generally considered to arise from the reduction in surface energy due to decreasing the total surface area. Various mechanisms have been proposed for the necessary movement of material. Those most commonly considered are viscous flow, vaporization and subsequent condensation, diffusion through the lattice, and surface migration. The relative contributions of the different mechanisms have not been established, and evidently will vary greatly from system to system. Shaler[13] contends that metals must flow in order to densify, and that densification cannot progress by evaporation and condensation or by surface diffusion. In a review of the mechanism of sintering, J. P. Roberts[14] divides the process into two stages. The first stage is characterized by connected pores and the second stage by disconnected pores. Evaporation and condensation play a part in densification during the first stage, but contribute only to spheroidization of pores in the second stage. A flow mechanism is used to account for densification in the second stage.

In the investigation of sintering in powder metallurgy, the extent of densification is often used as a measure of the degree of sintering. Eitel[15] uses such a definition. Densification, however, is only a manifestation of one of the many changes taking place in the physical and chemical properties of ferrites during sintering.

2.1.3 Grain Growth. The grain growth in metals is fairly well under-

stood. The literature contains a small amount of information on the grain growth of oxide systems. In the process of grain growth, the larger grains grow at the expense of the smaller grains and the surface energy is reduced. Wilder and Fitzsimmons[16] found that grain growth in Al_2O_3 occurs predominantly after the densification is complete. We have found in Ni-Zn ferrites that grain growth and densification occur simultaneously.

The influence of the grain size on the magnetic properties of alloys has been investigated at various times and a correlation of permeability and grain size is usually found. Walters[17] found a correlation of permeability and grain size in an alloy containing nickel, iron, copper and molybdenum. An investigation of grain size in ferrites and its influence on the magnetic properties is in progress at this laboratory and will be reported later.

2.1.4 The Diffusion Process. The diffusion here considered is that which homogenizes the formed spinel. It is conceivable that the local composition could vary greatly in the initially formed spinel. These local differences would be removed by a diffusion process. This process is to be considered independently of other diffusion processes active in (1) formation of the spinel, (2) bulk densification, and (3) grain growth.

The part played by diffusion in this respect would depend upon the extent of premixing of the oxides. This can be varied over an extremely wide range. The two extremes that could be considered are the placing of two layers of different oxides together and the intimate mixing presumably obtained by coprecipitating the reacting materials. Surely the role played by diffusion in obtaining a homogeneous material would be different in the two cases.

2.2 The Effect of Manufacturing Procedure on the Magnetic Properties of the Ferrite Core

2.2.1 Properties Related to Raw Materials. The reactivity of the mixed oxides would be expected to be dependent upon the particle size of the oxides used. The particle size would determine the limit of mixing that could be obtained. Assuming that the particles are completely mixed, the area of contact between the component oxides would be limited by the particle size of the oxides. Coprecipitation from a basic solution of the hydroxides or salts of the material being used would remove this limitation and will be considered later.

The method of preparation of the oxides used has been shown to influence the reactivity of the material. Hopkins[9] has shown that the reactivity of Fe_2O_3 with ZnO to form zinc ferrite is greatly influenced by the temperature of preparation of the Fe_2O_3. Hedvall[18] has shown that the salt from which the Fe_2O_3 is prepared changes the reactivity of the oxide.

The purity of the oxides would also be expected to influence the properties of the final material. It has been shown in this laboratory that the addition of small amounts of V_2O_5[19] as a flux lowers the reaction temperature by as much as 400°C.

In the experiments reported here, no attempt was made to investigate the relative contributions of the above to the finished material. The oxides from which the cores were made were held constant, with the exception of the work done on coprecipitation. All oxides used were from Baker and labeled C.P. The particle size is given below, as determined by the Carboloy Company.

Oxide	Particle Size
Fe_2O_3	.26 Microns
ZnO	.58 Microns
NiO	.64 Microns

2.2.2 The Mixing Procedure. The method of mixing the reacting material would be expected to be a factor influencing the properties of the final product. There are two methods in general use. The most common method consists of ball milling the oxides in a liquid slurry. The second method is to coprecipitate the metallic ions from solution as the hydroxides or carbonates. The latter method ideally gives more intimate mixing than could be obtained by any mechanical mixing of the oxides, but is time consuming. It also creates new problems, such as washing out impurities which have been introduced into the precipitate, and insuring complete precipitation of the material.

Okamura and Simorzaka[10] have shown that the reaction mechanism is determined by the method of mixing. L. I. Rabkin[20] states that it has been shown that nearly identical properties can be obtained by various procedures using a proper choice of firing schedules. It would appear, however, that if the magnetic properties are the result of a summation of changes, such as outlined in section 2.1 and if these changes have different activation energies which are dependent on the properties of the green core, then only the equilibrium value would be independent of the method of preparation. The path followed in reaching this final state would be expected to be different in the various preparations. Some results of investigations on the effect of the mixing procedures are given below.

2.2.2.1 Mixing by Ball Milling. The ball mill used consists of a case hardened steel mill in which are placed hardened steel balls of varying size. The speed of milling was held constant at all times. Any results reported here might be affected by ball size distribution, ratio of oxides to liquid, and speed of milling, such that the optimum conditions would have to be obtained for the individual equipment used. However, the results should be in qualitative agreement

with any ball milling equipment.

During the ball milling process the oxides are dispersed and intermixed. Probably two processes occur; that is, the oxides are intermixed and the particle size is reduced. The extent of particle size reduction is not known, but it is to be expected that the intermixing of the already quite small particles is the dominant process.

The effect of ball milling for different lengths of time has been investigated. Figure 3 is a plot of the real permeability μ_1 vs firing temperature for cores prepared from material ball milled 10 minutes and 24 hours. It can be seen that the magnetic permeability is considerably higher for the longer ball milling time.

A number of cores were prepared from material ball milled 6 and 24 hours. Table (1) gives this data. It can be seen that the longer ball milling time results in a greater uniformity among cores and a slightly higher value of μ_1. If the magnetic permeability is used as a measure of the extent of reaction, it must be concluded that greater mixing increases the reaction rate.

Table (1)

	μ_1		μ_2	
Ball Mill Time (Hrs.)	Ave.	Std.Dev.	Ave.	Std.Dev.
6	846	115	266	106
24	886	61	264	61

The ferrous iron content is shown in Figure 4 as a function of firing time for cores prepared from material ball milled 10 minutes and 6 hours. Ferrous iron content in the 6 hour material decreases much more rapidly than it does for the material ball milled for a shorter length of time. This is taken

FIG. 3

EFFECT OF BALL MILLING TIME ON μ_1 & Q FOR $Ni_{.4}Zn_{.6}Fe_2O_4$

FIRING TIME 4 HOURS
FREQUENCY 2 MC

FIG 4

FERROUS IRON CONTENT VS FIRING TIME FOR A STOICHIOMETRIC NICKEL-ZINC FERRITE

(FIRED AT 1210°C)

to mean that the formation of Fe_3O_4 due to poor distribution of the NiO and ZnO is maintained over a longer period of time and that the extent of diffusion necessary to make the material homogeneous is greater in the poorly mixed material.

2.2.2.2 Mixing by Coprecipitation. The chloride salts of Ni, Zn and Fe in the proper stoichiometric amounts were dissolved in distilled water and coprecipitated with Na_2CO_3. The precipitate was filtered, washed free of chlorides and carbonates, and dried at 350°C. Cores were pressed from this material and fired at the temperatures of 600°, 800°, 900° and 1100°C. Figure 5 shows the permeability of these cores together with those of a group of cores with the same composition from ball milled material. It is seen that at any given firing temperature the coprecipitated material always shows the higher permeability. If one compares the permeability spectra of two cores formed respectively from coprecipitated and ball milled materials then fired together, the coprecipitated core is seen to behave in every way like a ball milled core fired at a higher temperature. It can be assumed from this that the coprecipitated material is more reactive than the ball milled material. It is known that when a solution of $FeCl_2$ and $FeCl_3$, formed by dissolving magnetite in HCl, is precipitated as the hydrous oxides and dried at 100°C, that the precipitate is magnetic. Okamura, Simorzaka and Torizuka[21] also report the formation of magnetic hydrous oxides by coprecipitation of ferrous and ferric ions and of cobalt and ferric ions. They state that the reactions occur as low as 100°C. Milligan and Holmes[22] have made a similar study of cupric ferrite.

The formation of magnetic ferrous ferrite has been repeated in this laboratory. It was found that the black hydrous oxides were magnetic before drying. Coprecipitated 20-30-NiZn ferrite was found not to be magnetic when first

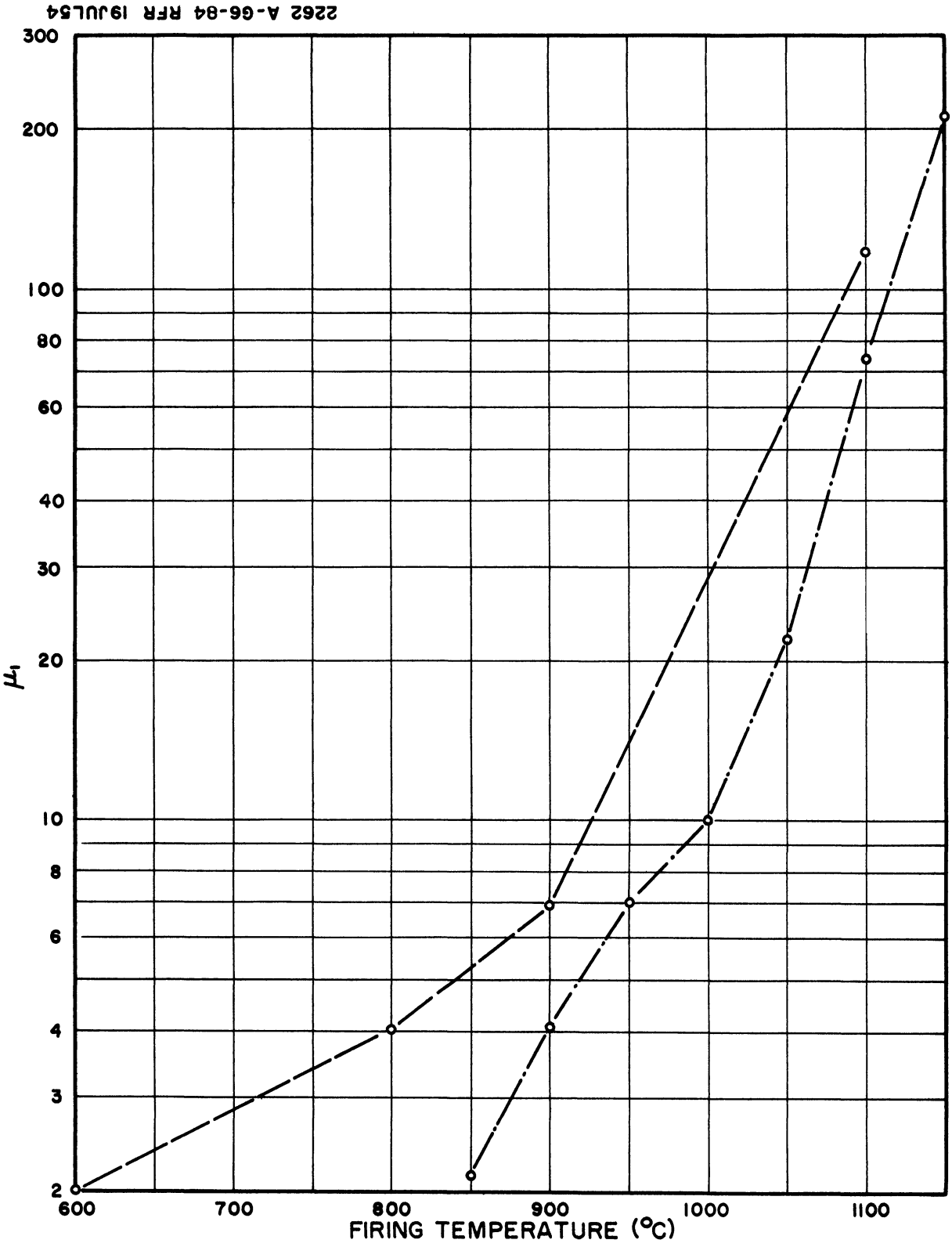

FIG 5
EFFECT OF MIXING METHOD UPON REAL PERMEABILITY

MIXING METHOD:

COPRECIPITATION ——— ———
BALL MILL —·——·—
FIRING TIME FOUR HOURS

formed, but became slightly so after several days. X-ray diffraction data show that the spinel formation begins at low temperatures. Figure 6 shows the powder patterns of material fired at 120°, 350°, and 1200°C for four hours. The pictures for 350° and higher show only the spinel lines, broad at 350° but sharp at 1200°C. The extra lines visible in the 120°C core are due to the presence of the separate metallic oxides.

The complete absence of the oxide lines seems to indicate that the reaction leading to spinel formation is complete even at 350°C. However, the lines are very broad and the material still has the physical appearance of the unreacted oxides. It is red, not fused together and soft. In addition, the permeability is only slightly higher for a given firing temperature than it is for the ball milled materials.

The explanation of this behaviour may lie with the phenomenon called mutual protective action. It is reported[23,24] from x-ray diffraction studies of hydrous oxide systems that two regions of concentrations are found in which the crystallization of one oxide is prevented by the other, and further that the effect is sensitive to temperature.

This work is further evidence that the magnetic properties of the ferrite are not determined completely by any one step in the progress toward the final form.

2.2.3 The Pressing Operation.

2.2.3.1 Formation of the Green Core. Since the solid state reaction involved in the preparation of ferrites depends upon intimate contact of the reacting oxides, the reaction should depend upon core compactness. The most common method of forming the core, and the method used in this laboratory, consists of pressing the oxides in a die, using a hydraulic press to apply the pressure. There are

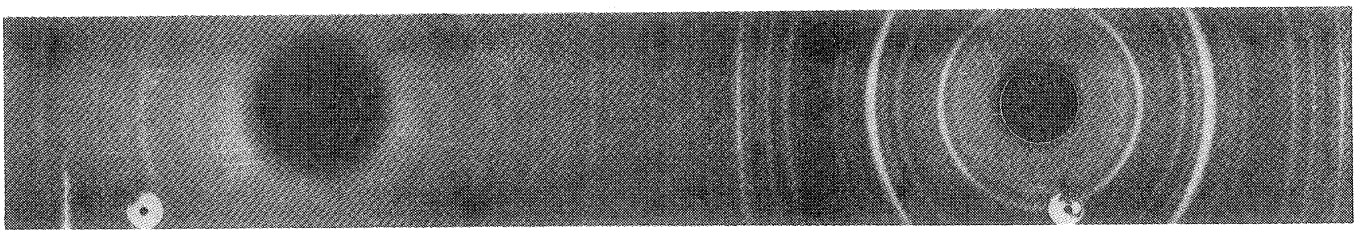

A. FIRING TEMPERATURE: 120°C

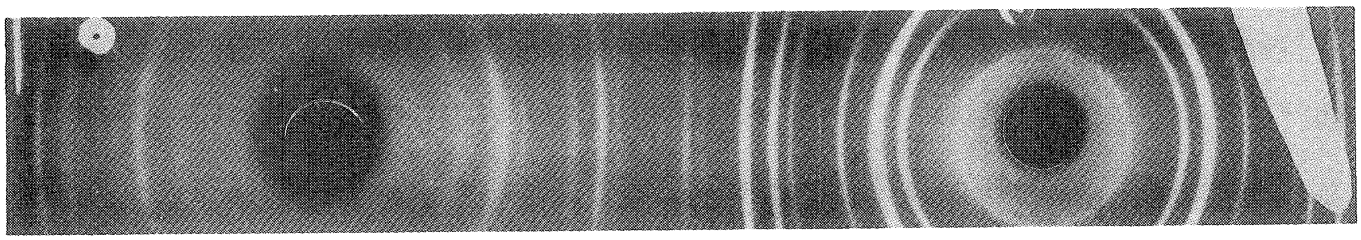

B. FIRING TEMPERATURE 350° C

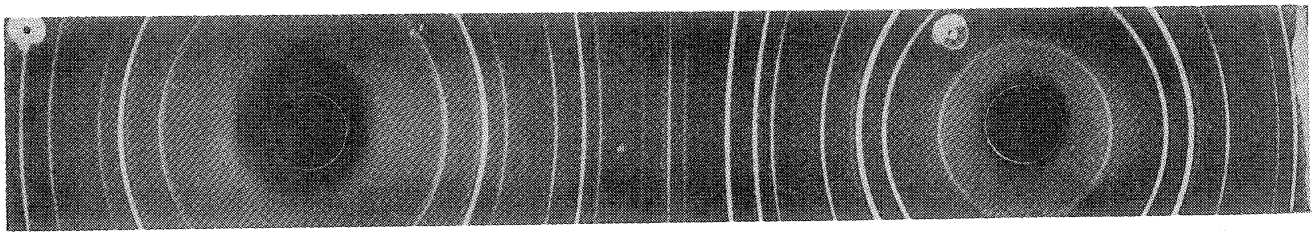

C. FIRING TEMPERATURE: 1200° C

FIG 6
X-RAY POWDER PHOTOGRAPHS
20-30 Ni-Zn; COPRECIPITATED
FIRING TIME 4 HOURS

A shows both oxide and spinel lines. B and C show only spinel lines. Note the relative sharpness of B and C

other methods, such as extrusion and hot pressing. Extrusion methods involve apparatus not available in this laboratory. Hot pressing also requires special equipment and was not attempted.

The use of oil on the die to reduce friction is recommended by Seelig[25] It was found unnecessary to do this if the die surfaces were wiped clean after each pressing. In the beginning a slip-fit was maintained between the working parts of the die. It was thought that this type of fit would not permit the oxides to work up between the sliding parts. This did not prove to be the case, however, and better results were obtained using a slip fit with about .005" clearance. A drawing of the die is given in Figure 7. The core OD is one inch, the ID about 0.6 inches.

It is sometimes convenient to press the cores well in advance of firing. It was found, however, that after the pressed green core stood a day or so, it cracked when fired. It was thought that the core might pick up moisture which cracked the core when driven off, but this did not seem to be the case. In any event, it was found desirable to press the cores just prior to firing.

2.2.3.2 Effect of Variation in Green Density on the Fired Ferrite Core. In order to evaluate the effect of the green density on the properties of the ferrite core, two investigations were conducted. In one case the firing time was held constant at four hours, and cores with different green densities were fired at a number of temperatures. In the other case, the effect of firing time was investigated at constant temperature for two different green densities.

The cores were made as follows. The oxides were ball milled for 6 hours in a liquid slurry using the above described hardened steel ball mill with steel balls. The liquid was removed by evaporation and the oxides were dried at 110°C. The dried material was then crushed and passed through a 200 mesh sieve.

FIG 7

FERRITE DIE

Cores were then pressed to obtain varying green densities by varying the pressing pressure. The cores fired at constant time and temperature with varying green density were ball milled in water, those fired at constant temperature were ball milled in acetone.

The cores fired at constant time were placed on 3" x 6" alundum trays, 14 cores to a tray, with three trays stacked together. The furnace was then brought to the desired temperature and held 4 hours. The cores were then cooled in oxygen at the rate of 60°C/hour. The cores fired at varying times were fired in alundum crucibles. Two cores with different green densities were placed in the furnace at the specified temperature, and withdrawn and air cooled. The data are given in Tables (2) and (3).

With sufficiently high firing temperature and a constant firing time, it is to be expected that the final density will approach the x-ray density for any reasonable value of green density. Similarly, at sufficiently low firing temperatures there will be no reaction and the final density will equal the green density. If the difference ΔD between the final density and the green density is plotted against the green density GD (each normalized by division by the x-ray density), these two limits would be represented by the two solid lines in Figure 8.

An unnormalized plot of the change in density as a function of the green density is given in Figure 9 for material fired for four hours. It can be seen that for intermediate temperatures the increased shrinkage of the lower density cores becomes smaller such that at 1000°C ΔD is independent of the compactness of the core.

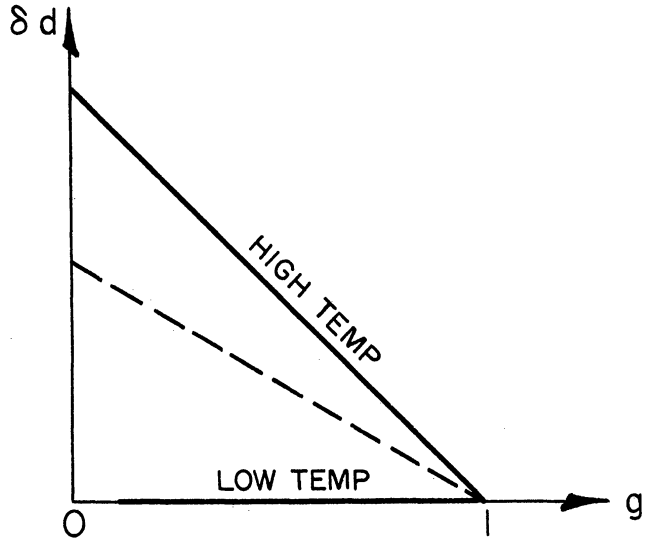

FIG 8

EXPECTED BEHAVIOR OF
DENSITY CHANGE UPON FIRING

Figure 10 shows the change in density as a function of the firing time. While in Figure 9 the cores with the smallest green density had the most shrinkage, in Figure 10 it can be seen that in the early stages of sintering the cores with the highest densities shrank the most. A plot similar to Figure 9 for a firing time of less than 80 minutes would have a positive slope at 1150°C.

The effect of varying green density on the magnetic permeability is difficult to evaluate from the data in Table (2). While there is a trend toward a higher permeability with increasing green density, there is too much scatter in the data to obtain a good correlation. The data at 1100° and 1150°C indicate that a large temperature variation existed in the furnace. This appears to have masked the effect due to the green density.

The correlation between green density and permeability is more clearly seen in Table (3) where the effect of temperature variation in the furnace was controlled by firing the core in the same location in the furnace. Figure 11 is a plot of μ_1 vs time for cores pressed to two different green densities. The permeability of the cores within the higher green density have higher permeabilities throughout.

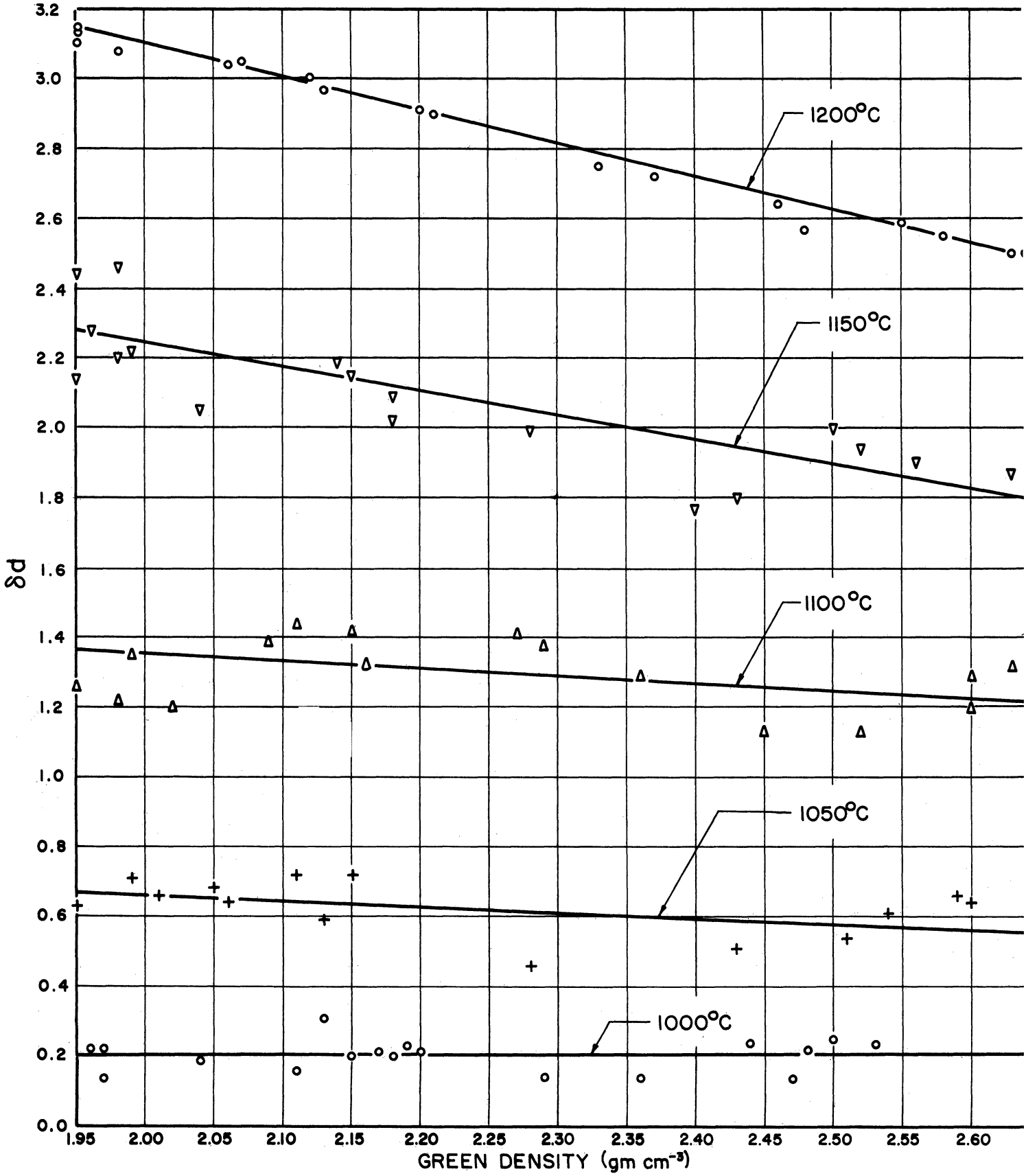

FIG 9
CHANGE IN DENSITY VS GREEN DENSITY FOR SEVERAL FIRING TEMPERATURES. FIRING TIME 4 HOURS
δd = FINAL DENSITY - GREEN DENSITY

FIG 10. CHANGE IN DENSITY VS FIRING TIME

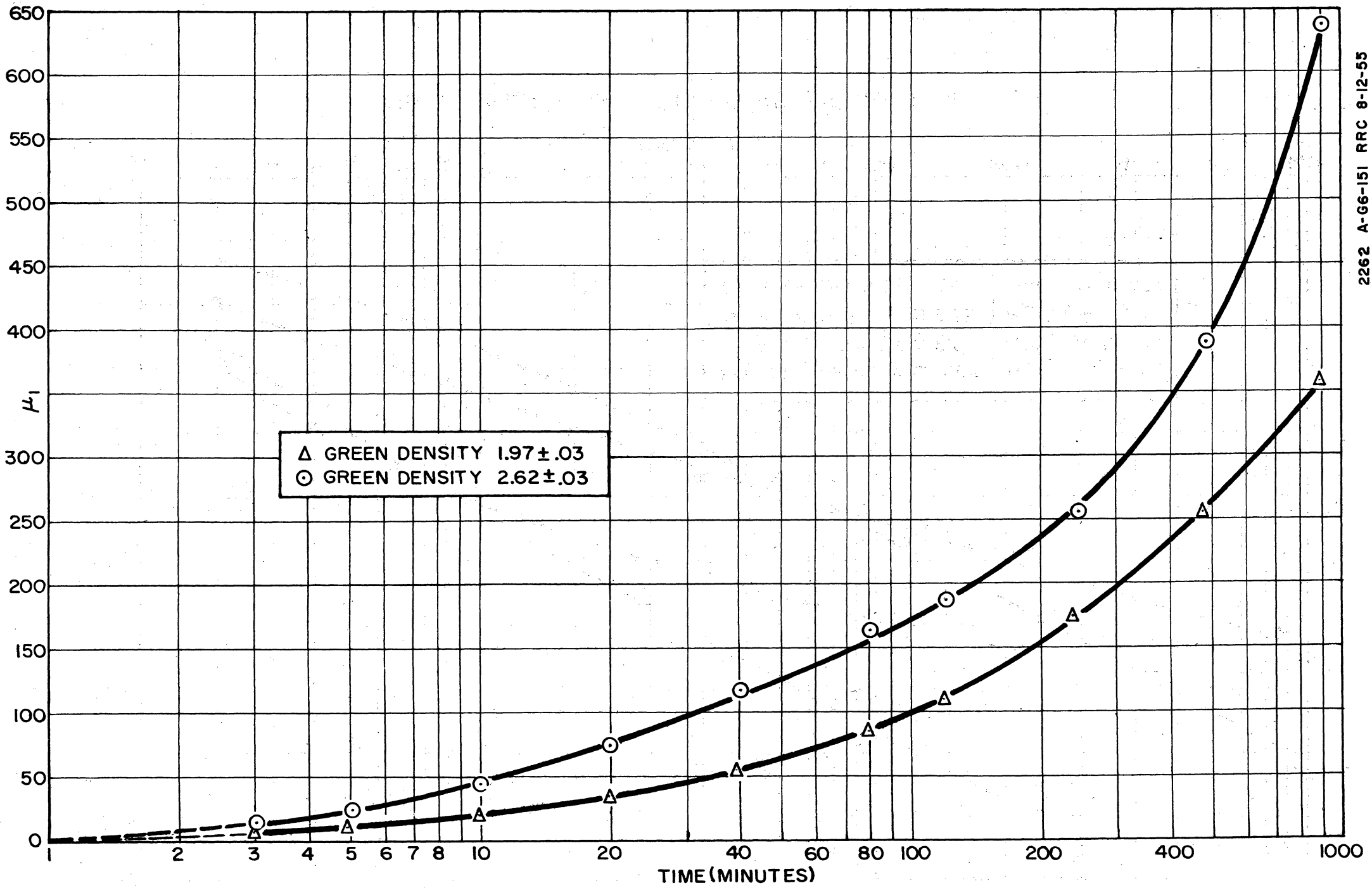

FIG 11. EFFECT OF GREEN DENSITY ON THE CHANGE IN μ_1 WITH FIRING TIME FOR $Ni_{.4}Zn_{.6}Fe_2O_4$ (FIRED AT 1150°C) FREQUENCY 2MC

TABLE (2)

Effect of Green Density on Properties of Cores—Firing Time 4 Hours

T = 1000° C

Green Density	Final Density	Δ.D.	μ_1 (2 mc)	Q (2 mc)
1.97	2.11	.14		
2.11	2.27	.16		
2.17	2.38	.21		
2.15	2.35	.20		
1.96	2.18	.22		
2.20	2.41	.21	no data	
2.19	2.42	.23		
1.97	2.19	.22		
2.18	2.38	.20		
2.04	2.23	.19		
2.29	2.43	.14		
2.36	2.50	.14		
2.47	2.61	.14		
2.13	2.54	.31		
2.44	2.68	.24		
2.50	2.75	.25		
2.48	2.70	.22		
2.53	2.77	.24		

T = 1050° C

Green Density	Final Density	Δ.D.	μ_1 (2 mc)	Q (2 mc)
1.99	2.70	.71		
2.13	2.72	.59		
1.94	2.57	.63		
2.06	2.70	.64		
2.15	2.87	.72		
2.11	2.83	.72	no data	
2.28	2.74	.46		
2.43	2.94	.51		
2.51	3.05	.54		
2.54	3.15	.61		
2.59	3.25	.66		
2.60	3.22	62		
2.05	2.73	.68		
2.01	2.67	.66		

T = 1100° C

Green Density	Final Density	Δ.D.	μ_1 (2 mc)	Q (2 mc)
2.02	3.22	1.20	52	13.8
1.99	3.34	1.35	61	64
1.92	3.18	1.26	52	72
1.98	3.20	1.22	46	92
2.11	3.55	1.44	79	68
2.09	3.48	1.39	72	69
2.15	3.57	1.42	76	75
2.16	3.49	1.33	66	61
2.27	3.68	1.41	87	64
2.29	3.67	1.38	88	62
2.36	3.65	1.29	75	33
2.45	3.58	1.13	65	78
2.52	3.65	1.13	66	75
2.60	3.80	1.20	98	72
2.60	3.89	1.29	114	66
			118	87
2.63	3.95	1.32	116	35
2.66	3.85	1.19	107	76

TABLE (2) (Continued)

T = 1150° C

Green Density	Final Density	Δ.D.	μ_1 (2 mc)	Q (2 mc)
1.96	4.24	2.28	295	45.6
1.92	4.36	2.44	350	27.1
1.98	4.44	2.46	385	34.4
1.92	4.06	2.14	189	33.7
1.99	4.21	2.22		
1.98	4.18	2.20	235	27.5
2.18	4.20	2.02	238	35.3
2.04	4.09	2.05	191	28.4
2.18	4.27	2.09	253	37.1
2.15	4.30	2.15	251	37.1
2.14	4.33	2.19	236	24.2
2.28	4.27	1.99		
2.40	4.17	1.77	178	51.9
2.43	4.23	1.80	181	39.
2.52	4.46	1.94	273	24.6
2.50	4.50	2.00	307	20.2
2.63	4.50	1.87	287	25.2
2.56	4.46	1.90	273	26.5

T = 1200° C

Green Density	Final Density	Δ.D.	μ_1 (2 mc)	Q (2 mc)
1.95	5.05	3.10	659	6.4
1.92	5.05	3.13	692	6.0
1.92	5.06	3.14	881	3.7
1.98	5.06	3.08	865	4.7
2.07	5.12	3.05	921	3.-
2.06	5.10	3.04	753	4.0
2.12	5.12	3.00	1014	2.7
2.13	5.08	2.87	813	4.2
2.21	5.11	2.90	788	3.73
2.20	5.11	2.91	943	2.6
2.33	5.08	2.75	872	3.1
2.37	5.09	2.72		
2.48	5.05	2.57	787	4.6
2.46	5.10	2.64	968	3.65
2.58	5.13	2.55	1030	2.78
2.55	5.14	2.59	1038	2.65
2.64	5.14	2.50	1086	2.20
2.63	5.13	2.50	1104	2.5

TABLE (3)

Effect of Firing Time on Properties of Cores — Constant Green Density

T = 1150° C

Green Density	Final Density	Δ.D.	μ_1 (2 mc)	Q (2 mc)	Time (Min.)	Green Density	Final Density	Δ.D.	μ_1 (2 mc)	Q (2 mc)
1.96	2.79	.828	8.2	35	3	2.64	3.65	1.01	16.1	38
1.97	2.94	.970	12.9	40	5	2.64	3.76	1.12	25.4	38
1.98	3.06	1.08	20.0	39	10	2.64	3.92	1.28	44	39
1.93	3.28	1.35	35.2	39	20	2.66	4.14	1.48	76	37
1.95	3.50	1.55	55.	40	40	2.65	4.32	1.67	117	37
1.96	3.76	1.80	86.	40	80	2.66	4.45	1.79	163	37
2.00	3.92	1.92	110.	41	120	2.60	4.52	1.91	187	38
1.99	4.23	2.24	118.	37	240	2.64	4.67	2.03	257	34
2.00	4.47	2.48	254.	39	480	2.62	4.84	2.21	389	25
1.92	4.66	2.74	358.	29	900	2.66	4.94	2.28	630	10

T = 1210° C

Green Density	Final Density	Δ.D.	μ_1 (2 mc)	Q (2 mc)	Time (Min.)	Green Density	Final Density	Δ.D.	μ_1 (2 mc)	Q (2 mc)
2.07	3.22	1.15	27	48	3	2.65	3.88	1.23	48	46
2.10	3.55	1.45	47	48	5	2.64	4.14	1.50	76	48
2.03	3.60	1.57	54	49	7	2.63	4.23	1.60	90	48
2.05	3.79	1.74	69	49	10	2.64	4.36	1.72	110	47
2.06	3.97	1.91	86	50	15	2.64	4.47	1.83	129	47
2.11	4.42	2.31	158	45	40	2.65	4.72	2.07	195	43
	4.59		180	44	60	2.64	4.79	2.15	212	41
2.06	4.64	2.58	199	39	80	2.65	4.85	2.20	264	32
2.00	4.75	2.75	233	35	120	2.66	4.94	2.28	306	23
1.99	4.93	2.94	286	20	240	2.64	5.01	2.37	368	12
			(296)	(13)						

The following facts have been observed:

(1) The rate of densification during the initial stages of sintering is higher for the more densely compacted material.

(2) The extent of densification of the material is a function of the green density, the firing temperature and the firing time.

(3) For a given temperature there is a time when the change in density is independent of the extent of compaction. From Figure 9 and 10 this time is 10 minutes at 1210°C, 80 minutes at 1150°C and 240 minutes at 1000°C. Data represented as in Figure 9 would have positive slopes for material fired at less than these times at the representative temperatures.

(4) For any given firing time, the magnetic permeability is increased by increasing the green density of the cores.

2.2.4 The Firing Procedure. One of the most important processes in the preparation of ferrites is the firing procedure. The number of variations that can be made in this one procedure alone is so large that it cannot be hoped to cover all of them in one report. No attempt has been made to do this. The best that can be hoped for is to hold the main firing procedure constant while varying one factor at a time. Some of the variables that might be considered are firing time, firing temperature and annealing temperature. A Harper electric furnace, Model HL6, was used. It is a glo-bar furnace with a temperature range of 0-1500°C. The temperature was maintained with a Plat. vs. Plat. + 10% Rhodium thermocouple and a Brown balancing potentiometer manufactured by the Minneapolis-Honeywell Regulator Company.

The rate of a reaction is known to be greatly accelerated by increasing the reaction temperature. Okamura[21] found that the magnetic moment of $NiFe_2O_4$ increased rapidly to a limiting value at a given temperature and then remained

constant. Guillisen[8] found what appeared to be an equilibrium value in the extent of reaction of $ZnFe_2O_4$ at a given temperature. Measurements made in this laboratory are presented in Figures 12 through 15. Figure 12 shows the effect of increasing the firing temperature on the magnetic permeability and Q value. The firing time was held constant at 4 hours. Figure 13 is a plot of the density vs the firing temperature for the same cores. It can be observed that the densification and permeability start to increase at about the same firing temperature.

Figure 14 shows the change in μ_1 and Q as a function of firing time at two firing temperatures. It can be seen that the magnetic properties of the cores fired at 1262° and 1212°C are identical at 16 minutes firing time and 78 minutes firing time respectively. For a given value of μ_1 the $\mu_1 Q$ product is relatively constant for the two firing temperatures.

The grain growth at 1210°C is shown in Figure 15. It can be seen from this and Table (3) that the densification and grain growth progress together.

The rate at which the ferrite is cooled from the firing temperature would be expected to change the magnetic properties of the material. In general it would seem most desirable to cool slowly, since the material would undergo less thermal shock. Slow cooling would also permit the cations to approach equilibrium positions among the A and B lattice sites. It has been reported[26] that $ZnFe_2O_4$ is ferromagnetic when quenched from 1400° due to some of the zinc cations being maintained on the B sites during the quenching. Slowly cooled $ZnFe_2O_4$ has the normal spinel structure.

In nonstoichiometric ferrites containing ferrous iron, the rate of cooling, along with the extent of densification, determines the extent of oxidation of the ferrous iron. This was found to be of importance in evaluating the effect of ferrous iron on the magnetic properties of the ferrites and is reported on in section 3.

FIG. 12

COMPLEX INITIAL PERMEABILITY VS FIRING TIME, 2MC

$[Ni_{.4}\ Zn_{.6}\ Fe_2O_4]$

FIG 13

DENSITY VS FIRING TEMPERATURE

$[Ni_{.4}\ Zn_{.6}Fe_2O_4]$

FIRING TIME 4 HOURS

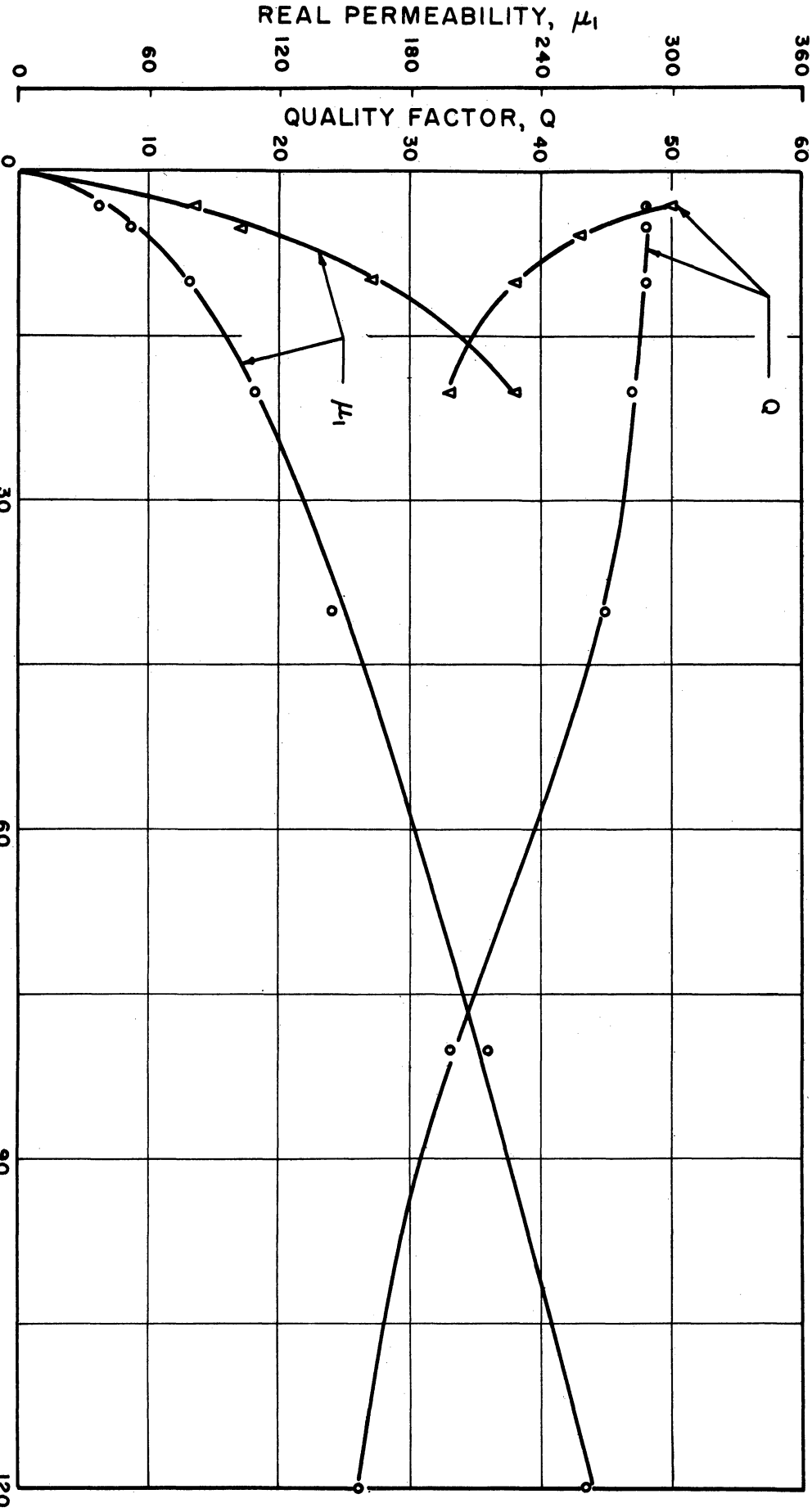

FIG. 14. μ_1 AND Q VS FIRING TIME
$[Ni_{.474}Zn_{.526}Fe_2O_4]$
° 1212°C

2262 A-G6-117 RFR 25FEB55

FIRED FOR 40 MINUTES

FIRED FOR 80 MINUTES

FIRED FOR 120 MINUTES

FIRED FOR 180 MINUTES

FIRED FOR 240 MINUTES

FIRED FOR 900 MINUTES

FIG 15

GRAIN GROWTH IN Ni-Zn
FERRITE FIRED AT 1210°C
(X1000)

3. THE EFFECT OF FERROUS IRON ON THE MAGNETIC PROPERTIES OF NICKEL-ZINC FERRITES

3.1 The RO-Fe_2O_3 System

The system $ZnFe_2O_4$ was investigated by Kato and Takei[27]. They found that $ZnFe_2O_4$ + Fe_2O_3 was magnetic, while $ZnFe_2O_4$ was not and that the magnetic properties were due to two forms of iron oxide. In one case they concluded that $ZnFe_2O_4$ + magnetic Fe_2O_3 was formed and that the magnetic properties were due to the presence of magnetic Fe_2O_3 as a second phase. In the other case $ZnFe_2O_4$ + Fe_3O_4 was present with the Fe_3O_4 in solid solution with the $ZnFe_2O_4$.

On the other hand, Berger[28] investigated the same system and determined the solubility of Fe_2O_3 in zinc ferrite by measurement of the lattice constant. He found the limiting mole percentage of Fe_2O_3 in the spinel to be 76% at 1400°C, 64% at 1200°C, and about 61% at 1000°C. From density considerations he concluded that the spinel lattice containing excess Fe_2O_3 contained lattice holes. In other words the solid solution contained γFe_2O_3.

Kushima and Amanuma[29] investigated the system $ZnFe_2O_4$ by x-ray methods and by chemical analysis for Fe_3O_4. They attributed the magnetic properties of $ZnFe_2O_4$ containing excess Fe_2O_3 to the solubility of magnetic Fe_2O_3 with the zinc spinel. They found that some of the excess Fe_2O_3 was converted to Fe_3O_4, but concluded that the magnetic intensity was not due to the Fe_3O_4. Further, they gave a phase diagram for the system based on their x-ray data and chemical analysis.

The following is the report of an investigation of the formation of Fe_3O_4 in Ni-Zn ferrites and the effect of this formation on the magnetic properties of the material.

3.2 Preparation and Measurements of Samples

All material was prepared from C.P. oxides by ball milling the proper amount of NiO, ZnO and Fe_2O_3 in acetone for 6 hours. The acetone was then decanted and the oxides dried. The dried oxides were then crushed in an agate mortar and pressed into toroids. The toroids were fired in the Globar furnace in an air atmosphere.

Magnetic measurements were made on a Q-meter. Ferrous iron determinations were made by dissolving the ferrite in a standardized solution of .1N $SnCl_2$ in HCl under an atmosphere of O_2 free CO_2. The amount of ferrous iron was then determined by titration with $K_2Cr_2O_7$. The correction for the addition of $SnCl_2$ was determined by an identical analysis on a solution of $FeCl_3$ containing no ferrous iron. This procedure was adopted because the ferrite is difficult to dissolve in anything but the $SnCl_2$ solution.

The compositions investigated are given in Table (4).

TABLE (4)

Compositions Investigated

Composition	Moles ZnO	Moles NiO	Moles Fe_2O_3
1	.526	.474	1.000
2	.526	.474	1.135
3	.526	.474	1.294
4	.526	.474	1.570
5	.526	.474	1.938
6	.526	.474	3.000

These compositions correspond to the ferrite $Ni_{.474}Zn_{.526}Fe_2O_4$ with excess Fe_2O_3

in the ratio of moles Fe_2O_3 per mole ferrite of 0, .135, .294, .570, .938 and 2.000.

It was found that in order to determine the equilibrium value of ferrous iron, a very rapid quench was necessary. This was obtained by a water quench. The amount of oxidation during an air quench was found to depend on the looseness of the powder, or on the surface area exposed to the air. Table (5) shows the ferrous iron content of $Ni_{.474}Zn_{.526}Fe_2O_4 + .938\ Fe_2O_3$ cooled in various ways. The material fired as a loose powder and water quenched has the highest ferrous iron content. It might be that in the loose powder, the NiO and ZnO did not react completely to form the Ni-Zn ferrite. In this event, the high results would be expected.

Table (6) contains the data obtained by water quenching cores fired for various lengths of time at 1210°C. It can be seen that the % Fe^{++} is almost constant after 20 minutes firing time. It was concluded that water quenching was satisfactory.

TABLE (5)

Factors Influencing Extent of Oxidation During Cooling Process

$Ni_{.474}Zn_{.526}Fe_2O_4 + .938\ Fe_2O_3$ T = 1210°C

Material pressed into core	Cooling Method	Wt. % Fe^{++}
Core thickness .703 cm	Air cooled	3.39
Core thickness .107 cm	Air cooled	.72
Core thickness 1.66	Water quenched	6.32
Material fired as loose powder	Air cooled	.35
	Water quenched	6.85

TABLE (6)

Ferrous Iron Content of Material as Influenced by Firing Time

Water Quenched

$Ni_{.474}Zn_{.526}Fe_2O_4 + .938\ Fe_2O_3$ $T = 1210^{\circ}C$

Firing Time (Min.)	Wt. % Fe^{++}
3	5.29
5	6.34
10	6.31
20	6.44
900	6.55

3.3 Formation of the Ferrous Iron in Ni-Zn Ferrites

In the stoichiometric ferrite there appears to be two conditions leading to ferrous iron in the final product. The formation of ferrous iron below a temperature of about 1300°C is caused by the nonhomogenity of the material. The extent of ferrous iron formation in the material prepared at these temperatures is greatly influenced by the amount of mixing and the firing time. Figure 4 shows ferrous iron formation as a function of time for two different mixing procedures. The amount of ferrous iron in the well mixed material decreases with time. The amount of ferrous iron in the poorly mixed material also is decreased with time, but much slower.

The explanation of the formation of ferrous iron in ferrites at the lower temperatures appears to be as follows.

It is known that pure Fe_2O_3 does not form Fe_3O_4 in an oxygen pressure of 0.2 atmosphere below about 1390°C. However, as will be seen later, when NiO

and ZnO are present this temperature is considerably lowered.

The present study was carried out on a mixed nickel zinc ferrite of composition $Ni_{.474}Zn_{.526}Fe_2O_4$. To avoid duplication in the following discussion, R will be taken to indicate .474 Ni + .526 Zn .

The requirement for the formation of ferrous iron at 1210°C is that RO and Fe_2O_3 be present in a non-stoichiometric ratio. In a stoichiometric mixture the distribution of the oxides might be assumed to be as shown in Figure 16.

In the initial heating period, the spinel structure is formed and since the oxides are distributed in a non-stoichiometric ratio, ferrous iron is formed in the regions where the Fe_2O_3 is in excess. After prolonged heating, diffusion of the RO into the spinel results in the oxidation of the ferrous iron with the formation of more RFe_2O_4. Above 1300°C the formation of ferrous iron is due to the decomposition of the Ni-Zn ferrite. It is possible that the material becomes slightly non-stoichiometric due to volatization of zinc.

Ferrous iron is also formed in spinels when Fe_2O_3 is present in a greater mole fraction than RO at a temperature considerably below 1390°C. The formation of magnetite in such ferrites has been investigated. It is obvious that the presence of RFe_2O_4 stabilizes the ferrous iron. The magnitude of the effect is given in Table (7). The fraction of the excess Fe_2O_3 over RO converted to magnetite is shown in Figure 17.

Kushima and Amanuma have shown that there is a two phase area in the phase diagram of the Fe_2O_3-ZnO system where Fe_2O_3 coexists with Fe_3O_4 in solution with $ZnFe_2O_4$, bounded by a one phase area containing only the spinel structure. They found, as has been confirmed in this laboratory for the NiO-ZnO-Fe_2O_3 system, that magnetite was present in both areas. It is here proposed that in the two-phase area the amount of Fe_3O_4 present is determined by the solubility of

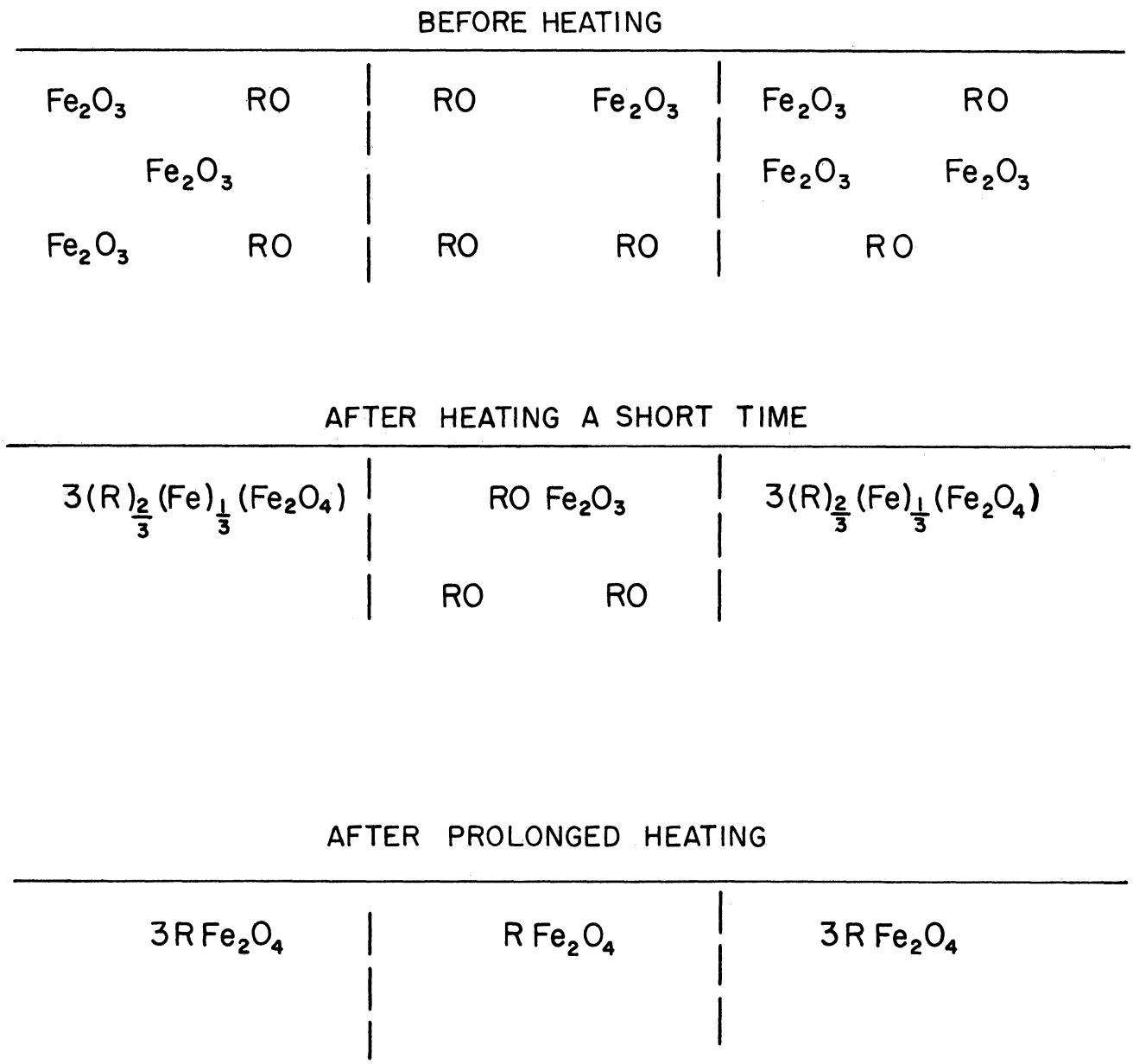

FIG 16

MECHANISM FOR THE FORMATION OF FERROUS IRON IN STOICHIOMETRIC FERRITES AT LOW TEMPERATURES

(IN THIS CASE "R" DOES NOT NECESSARILY REPRESENT .474Ni + .526Zn, BUT CAN BE ANY RANDOM MIXTURE OF THE TWO.)

FIG 17

FRACTION OF MAGNETITE FORMED AS A FUNCTION OF FIRING TEMPERATURE.

2262 A-66-130 CW 6-11-55
RED'N RRC 7-15-55

TABLE (7)

Ferrous Iron Content of Water-Quenched Cores

Temp.	1		2		3		4	
	% Fe^{++}		% Fe^{++}	Mole Fe_3O_4/ Mole ferrite	% Fe^{++}	Mole Fe_3O_4/ Mole ferrite	% Fe^{++}	Mole Fe_3O_4/ Mole ferrite
1000			.99	.050	.78	.054	.51	.051
1050			1.63	.083	1.14	.079	.90	.09
1100			2.82	.143	2.08	.142	1.50	.149
1150			3.13	.159	3.43	.237	2.48	.247
1200	.08		3.46	.175	5.99	.412	4.35	.431
1250			3.57	.180	7.41	.509	6.96	.688
1300	.16		3.71	.187	7.9	.542	10.91	1.07
1350			3.77	.190	8.31	.570	11.72	1.15
1400	.89		3.85	.194	8.54	.585	12.26	1.20
Theo-retical Limit			3.87	.196	9.13	.625	13.62	1.33

(1) $Ni_{.474}Zn_{.526}Fe_2O_4$

(2) $Ni_{.474}Zn_{.526}Fe_2O_4 + .294\ Fe_2O_3$

(3) $Ni_{.474}Zn_{.526}Fe_2O_4 + .938\ Fe_2O_3$

(4) $Ni_{.474}Zn_{.526}Fe_2O_4 + 2.0\ Fe_2O_3$

magnetite in the nickel zinc ferrite. In this region the moles Fe_3O_4 per mole of RFe_2O_4 appears to be constant at a given temperature and independent of composition. This can be seen in Table 7, where the moles of Fe_3O_4 per mole of RFe_2O_4 has been calculated from the ferrous iron content assuming all ferrous iron to be combined as magnetite. The equation for magnetite formation is:

$$A\ RFe_2O_4 + B\ Fe_2O_3 \text{ ------ } A\ RFe_2O_4 + (B - 3/2\ D)\ Fe_2O_3 + D\ Fe_3O_4 + D/2\ O_2$$

The moles of magnetite per mole of nickel zinc ferrite is then

$$\frac{D}{A} = \frac{\left(\left[RFe_2O_4\right] + \frac{B}{A}\left[Fe_2O_3\right]\right) \times \%\ Fe^{2+}}{100\left[Fe\right] + \left(\frac{3}{2}\left[Fe_2O_3\right] - \left[Fe_3O_4\right]\right) \times \%\ Fe^{2+}}$$

where $[\ \ ]$ represents the molecular weight.

The regions above the line in Table (7) are the regions where the moles of Fe_3O_4 per mole of RFe_2O_4 are constant at constant temperature.

A microphotograph of the two phase area is shown in Figure 18. This material fired at 1250°C has only one phase present, indicating that the change from one phase to two phases occurs somewhere between 1200 and 1250°C, in agreement with Table (7).

In the one-phase area $\gamma\ Fe_2O_3$, Fe_3O_4 and Ni-Zn ferrite appears as a solid solution. The amount of Fe_3O_4 is not then determined simply by its solubility in the Ni-Zn ferrite, but depends upon other factors. Work is being continued to confirm the phase diagram suggested above.

3.4 The Magnetic Properties of Ni-Zn Ferrites Containing Excess Fe_2O_3

There are a number of ways in which the extent of reduction of a ferrite can be controlled. One obvious way is to control the firing atmosphere.

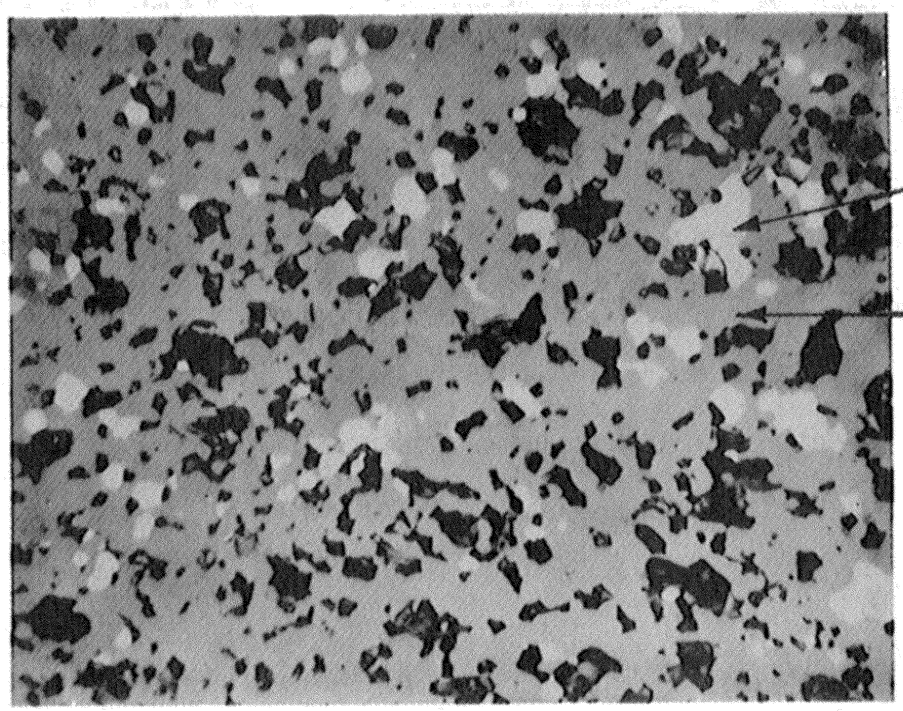

POLISHED, NOT ETCHED (X1000)

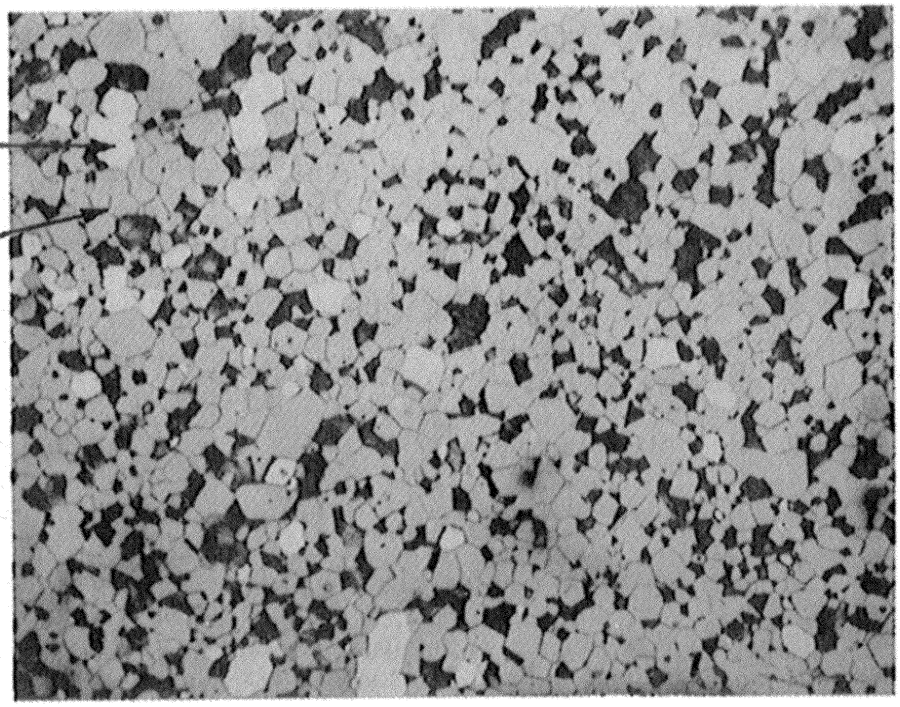

POLISHED AND ETCHED (X1000)

FIG 18 MICROPHOTOGRAPHS OF $Ni_{.474}Zn_{.526}Fe_2O_4$ +.938Fe_2O_3 FIRED FOR FOUR HOURS AT 1210°C AND AIR QUENCHED.

This would allow one to vary the ferrous iron content while holding the firing temperature constant. In this investigation, however, an air atmosphere was used during the firing and the extent of reduction of the Fe_2O_3 was varied by changing the firing temperature and the cooling procedure.

As stated above, it was concluded that water quench was rapid enough to maintain the high temperature composition of the core. When the material is air quenched, a considerable amount of oxidation takes place, the amount depending on the firing time. As the core becomes more dense, the ferrite is oxidized less during cooling in air.

The magnetic permeability and Q of five ferrites fired at 1210°C for varying lengths of time and air quenched in Figure 19 and Figure 20. It can be observed that μ_1 decreases and Q increases with increasing Fe_2O_3 content. This appears consistently throughout the investigation. Figure 21 and Figure 22 are surfaces showing the dependence of Q on firing time and frequency for a stoichiometric and non-stoichiometric ferrite. The former material has a maximum Q along the firing time axis, while the ferrite containing excess Fe_2O_3 has a maximum along both the frequency axis and the time axis.

Figure 23 is a plot of Q at 2 mc vs. % ferrous iron obtained from cores fired at several temperatures and air cooled. It can be observed that the value of Q increases to a maximum at about 3.5 % ferrous iron and then decreases. It appears that the maximum Q is determined by the concentration of ferrous iron.

Figure 24 is a plot of the ferrous iron content and Q at 2 mc. as a function of firing temperature for water quenched cores. If the Q depends only upon the ferrous iron content it would be expected that the drop in Q would be at the same ferrous iron content for the different heat treatments. This is not entirely true, although the Q starts to fall with the water quenched at a lower

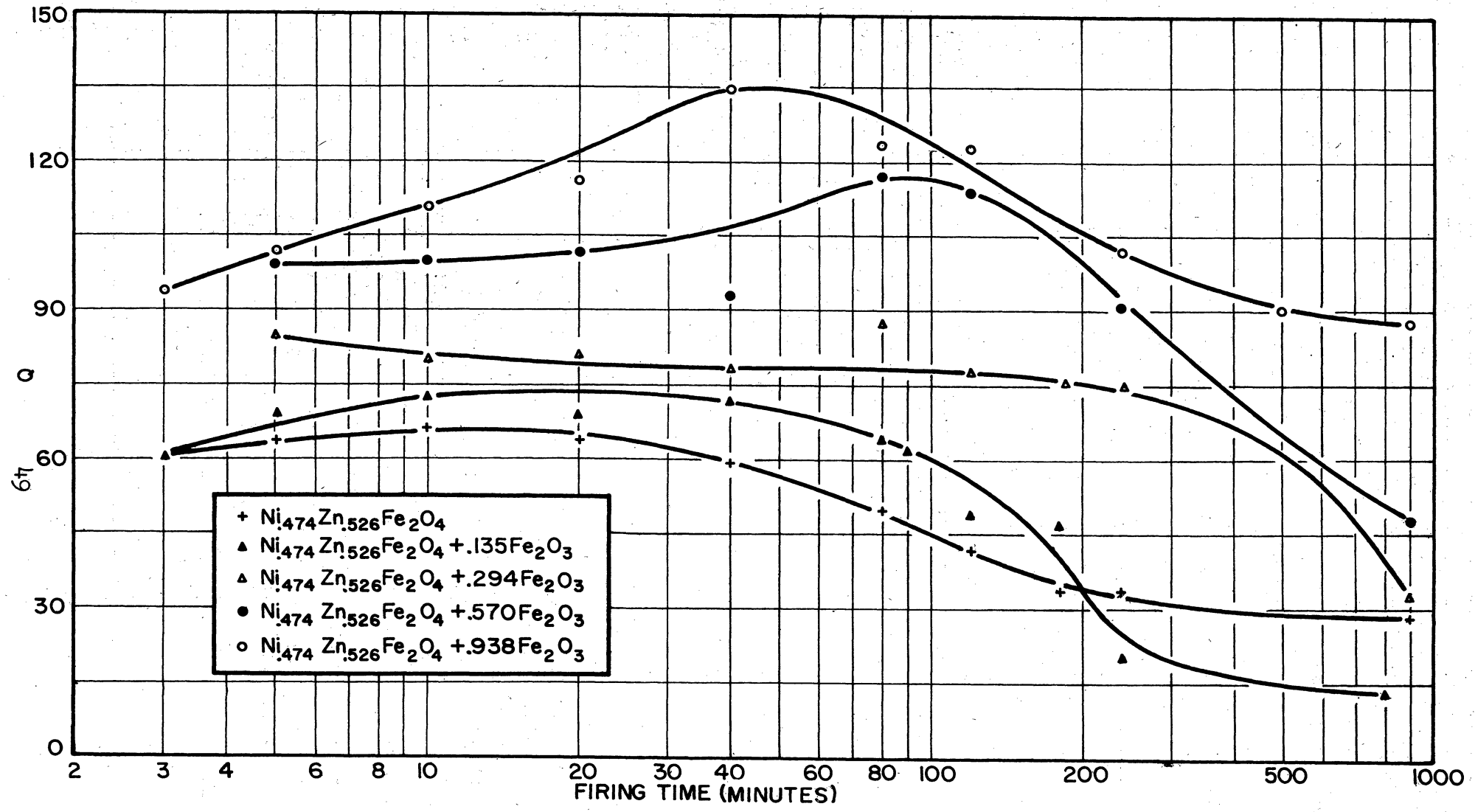

FIG 19

Q VS FIRING TIME FOR FIVE COMPOSITIONS
FIRING TEMPERATURE 1210°C
FREQUENCY 1 MC

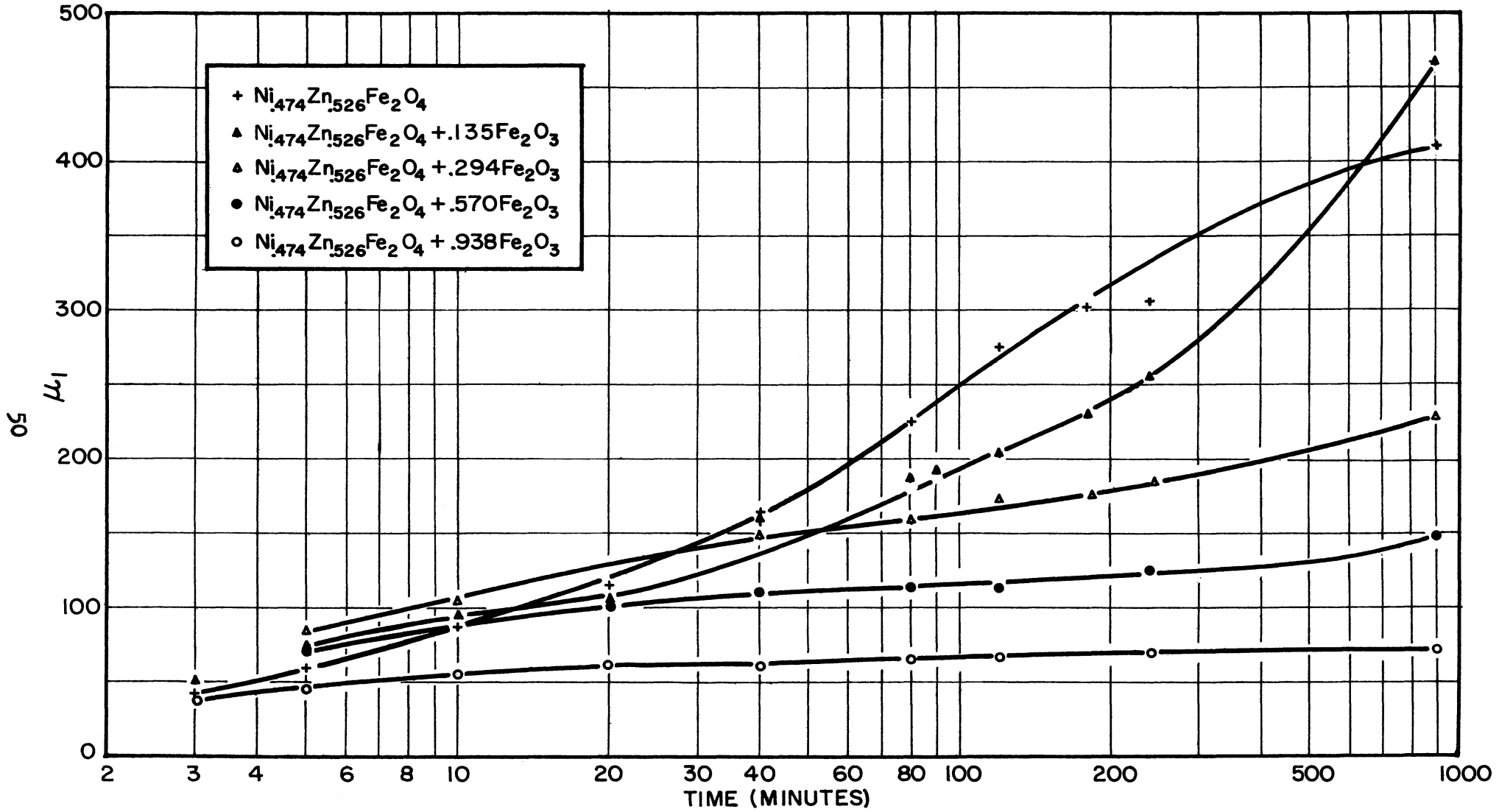

FIG 20

μ_i VS FIRING TIME FOR FIVE COMPOSITIONS

FIRING TEMPERATURE 1210°C

FREQUENCY 1 MC

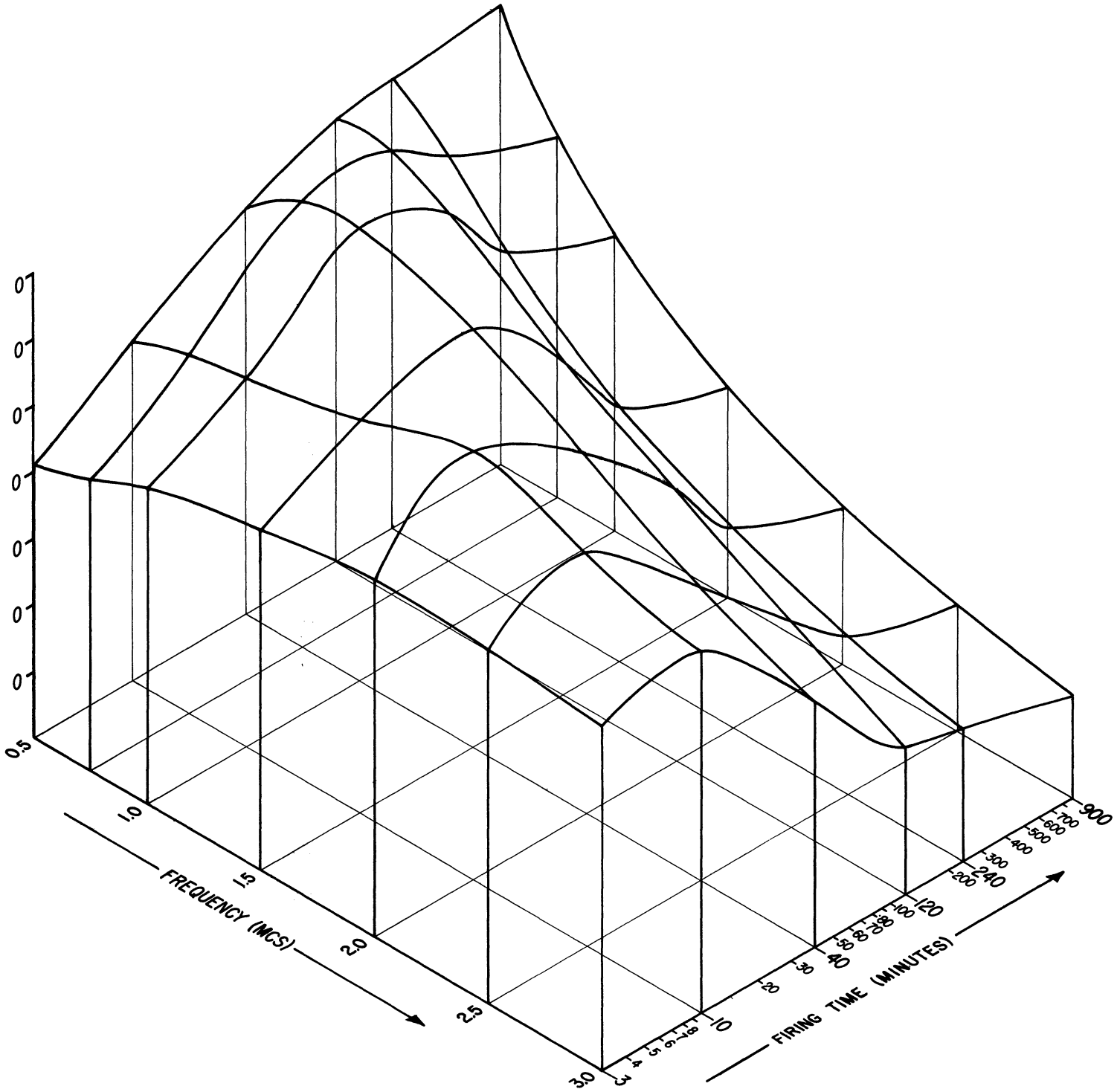

FIG 21

FREQUENCY-Q-FIRING TIME SURFACE

$Ni_{.474}Zn_{.526}Fe_2O_4+.938Fe_2O_3$

FIG 22
FREQUENCY-Q-FIRING TIME
SURFACE
$Ni_{.474}Zn_{.526}Fe_2O_4$

FIG 23 Q VS PERCENT FERROUS IRON
AIR QUENCHED
$[Ni_{.474}Zn_{.526}Fe_2O_4 + 938Fe_2O_3]$
FREQUENCY 2MC

FIG 24

Q AND PERCENT OF FERROUS IRON VS FIRING TEMPERATURE FOR WATER QUENCHED CORES

[$Ni_{.474}Zn_{.526}Fe_2O_4$+.938$Fe_2O_3$ —— FIRING TIME ONE HOUR]

FREQUENCY 2MC.

temperature than it does in the air quenched cores. It would be expected that the composition of the air quenched cores would not be uniform, since oxidation would be greatest at the surface. This might account for the observed result.

The magnetic properties of the core can be changed considerably by annealing. Data for 2 cores fired at 1210°C for 40 minutes and annealed at 800°C for 1 hour are given in Table (8). The stoichiometric core did not change, while there was a considerable change in the non-stoichiometric core. The non-stoichiometric core contained 3.1 % ferrous iron before annealing and .18% after annealing.

TABLE (8) at 2 mc

Effect of Annealing Under Oxidizing Conditions

	Before Annealing		After Annealing	
	μ_1	Q	μ_1	Q
$Ni_{.474}Zn_{.526}Fe_2O_4$	145	47	150	45
$Ni_{.474}Zn_{.526}Fe_2O_4$ + .938 Fe_2O_3	60	135	8.7	47

It was found that cores fired at higher temperatures were oxidized very little on annealing. It appears that if the core is dense, only a small amount of surface oxidation takes place. A frequency spectra of some cores before and after annealing is given in Figure 25. It can be seen that μ_1 is changed very little on annealing, but Q is increased, and the maximum is shifted to a higher frequency. Again the permeability decreases as the amount of Fe_2O_3 is increased. At the same time, the Q increases and the frequency at which the Q is maximum shifts to higher frequencies.

FIG. 25
FREQUENCY SPECTRA OF μ_1 & Q AS A FUNCTION OF TOTAL IRON CONTENT

The exact cause for the above occurrence is not known. If it were simply a metter of annealing out stresses, it would be expected to occur in the stoichiometric ferrite as well, which it does not. Evidently an orientation of the cations on different lattice sites is involved. The annealed material did not show a second phase in the polished sample.

The permeability of five compositions is given as a function of the firing time in Figure 20 at 2 mc. It can be observed that this value for $Ni_{.474}Zn_{.526}Fe_2O_4$ + .938 Fe_2O_4 reaches a constant value very early. All have increasing permeabilities with decreasing Fe_2O_3 content. It is apparent, at least in Composition 5, that the permeability is independent of the ferrous iron content, since this increases with time. This is borne out in Table (9) where the permeabilities of cores quenched in air and in water are given. Figure 26 shows the dependence of the permeability on firing time at 5 firing temperatures. Data showing the permeabilities and ferrous iron content are given in Table (10).

The Curie temperature for five compositions fired at 1210° and quenched in air is shown in Table (11). In two compositions the change in Curie temperature was investigated as a function of firing time. These data are given in Table (12). Both compositions show that the Curie temperature increases somewhat in the early stage of sintering and then remains relatively constant.

It has been observed throughout that as the Fe_2O_3 content is increased, the permeability is decreased. It was thought that the introduction of divalent iron into the lattice would effectively decrease the concentration of Zn and raise the Curie temperature. This could account for the lower permeability. Three compositions with varying zinc content were prepared and the magnetic properties and Curie temperature measured. Figure 27 shows the results of this experiment. While the Curie temperature increases with decreasing zinc content,

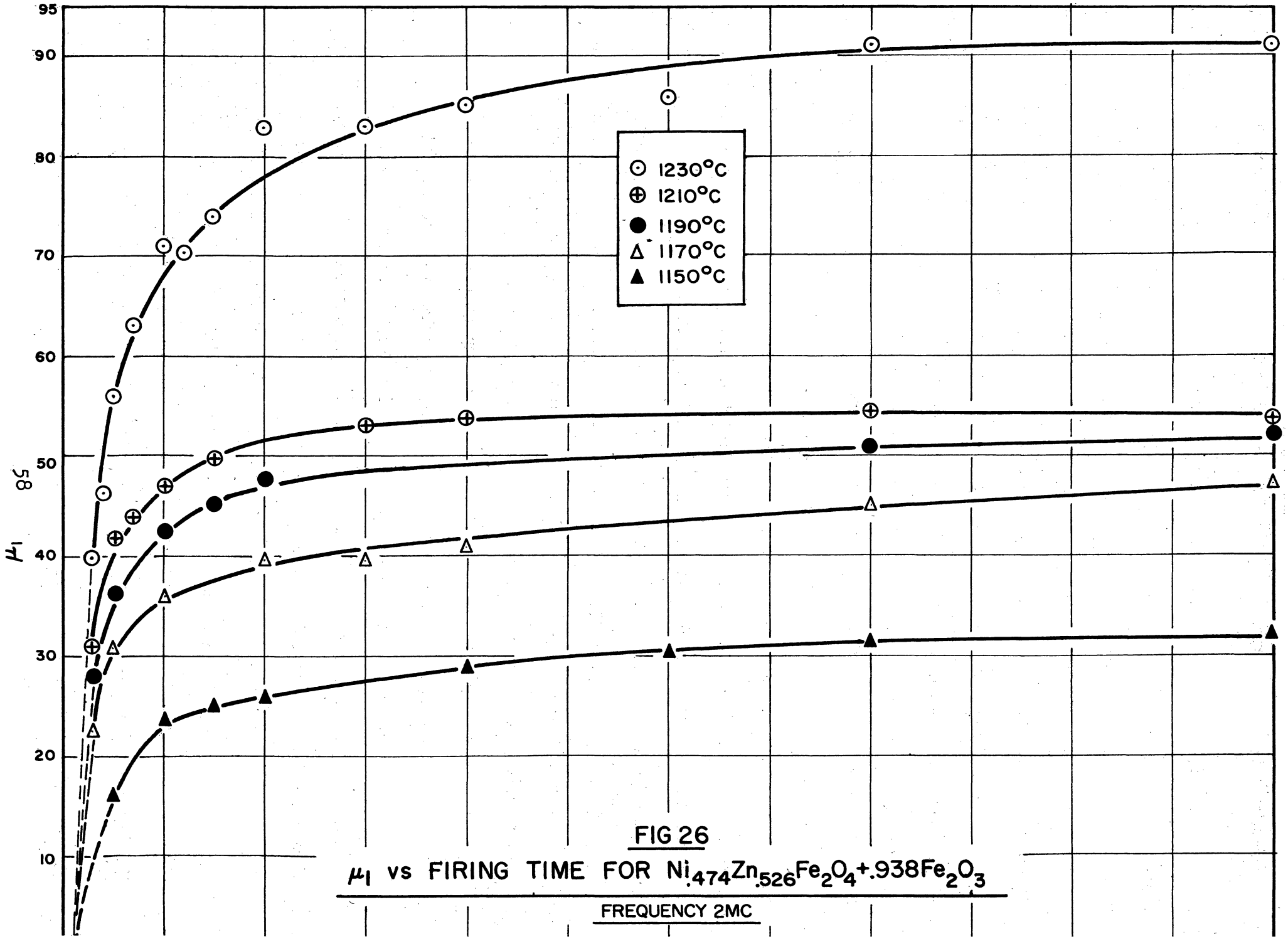

FIG 26

μ_1 vs FIRING TIME FOR $Ni_{.474}Zn_{.526}Fe_2O_4 + .938Fe_2O_3$

FREQUENCY 2MC

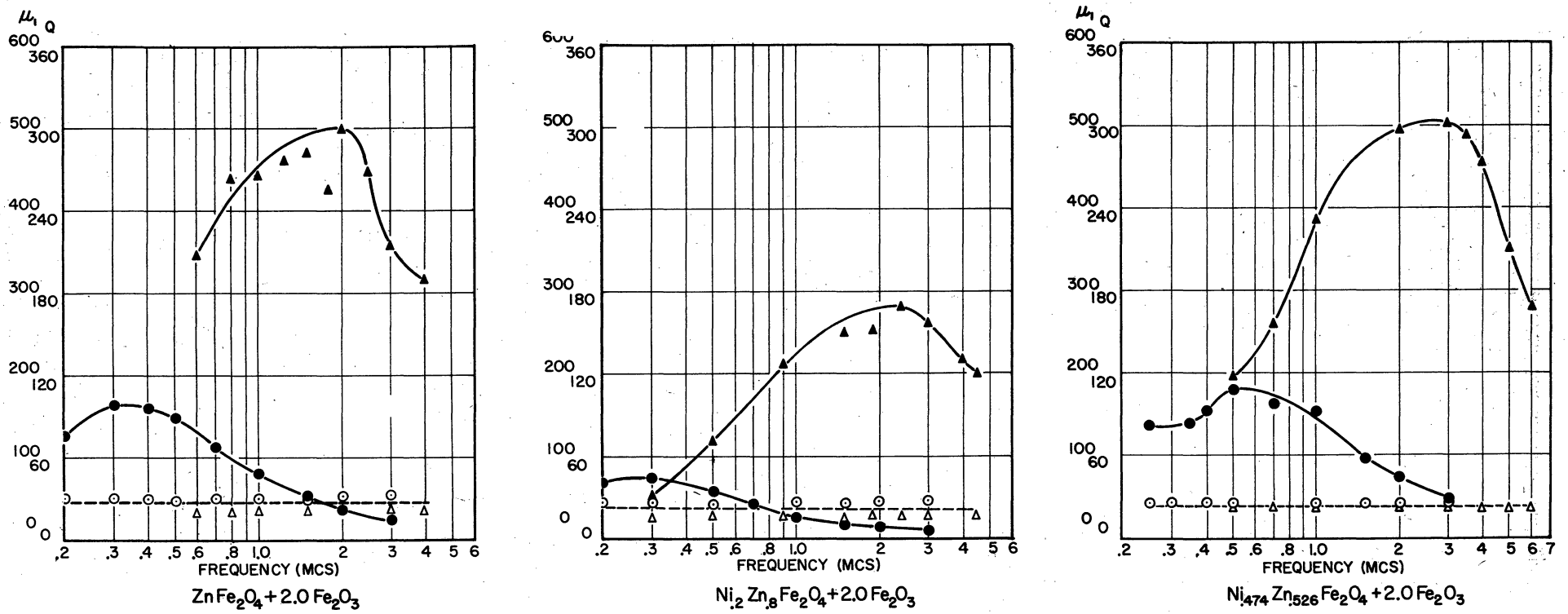

⊙ ● FIRED AT 1375°C FOR 1- HOURS

△ ▲ FIRED AT 1375°C FOR 1- HOURS & ANNEALED AT 800°C FOR 15 HOURS

● ▲ Q

⊙ △ μ_1

FIG. 27

EFFECT OF VARYING THE Ni-Zn RATIO ON MAGNETIC PROPERTIES OF A NON-STOICHIOMETRIC FERRITE

the permeabilities are almost equal. In order to understand this behavior, the phase diagram would have to be known.

TABLE (9)

Permeability Data for Water Quenched and Air Quenched Cores

Firing Temperature 1210°C

Firing Time (Min.) μ_1 (Water Quench) Comp. 5

Freq.	3	5	7	10	40	80	120	240	900
.9	32.2	39.9	44.0	49.5	55.9	56.5	27.4	57.5	58.5
2.0	33.8	42.0	46.4	52.3	59.0	59.9	60.3	60.7	62.35
4.0	34.2	42.5	46.8	54.7	59.8	60.8	61.2	62.2	63.44
7.0	35.1	43.4	47.6	53.9	61.7	62.8	62.8	63.4	65.7
12.0	33.8	41.8	46.7	53.4	60.5	62.8	61.8	63.0	64.8
18.0	36.9	46.4	51.7	58.9	67.3	69.9	70.3	72.4	74.4

Firing Time (Min.) μ_1 (Air Quench) Comp. 5

Freq.	3	5	7	10	40	80	120	240	900
.9	32.97	32.5		51.9	62.1	63.1	63.6	67.7	67.0
2.0	34.6	45.8		53.6	65.9	67.0	67.6	71.6	71.0
4.0	34.7	45.8		53.9	66.6	67.6	68.6	72.4	72.5
7.0	35.0	46.2		54.7	67.8	69.0	69.9	74.0	75.6
12.0	34.4	45.5		53.9	67.8	70.4	71.0	75.5	80.0
18.0	36.4	48.3		58.3	74.	77.9	81.5	87.3	93.6

TABLE (10)

Data on $Ni_{.474}Zn_{.526}Fe_2O_4$ + .938 Fe_2O_3 Fired Four Hours and Air Cooled

Temperature 1150°C

Core No.	Time (Min.)	μ_1 at 2 mc.	Q at 2 mc.	% Fe^{++}
A 439-1	5	15	91	.36
A 440-1	10	24	88	1.00
A 441-1	15	25	88	1.10
A 442-1	20	26	90	1.32
A 443-1	40	28	91	1.69
A 444-1	80	32	92	1.86
A 445-1	120	32	91	1.75
A 446-1	240	33	89	2.09
A 447-1	480	36	88	2.55
A 448-1	900	38	87	----

Temperature 1170°C

Core No.	Time (Min.)	μ_1 at 2 mc.	Q at 2 mc.	% Fe^{++}
A 392-1	3	23	92	.4
A 393-1	5	31	93	.94
A 394-1	10	36	101	1.35
A 396-1	20	40	106	1.62
A 397-1	40	41	108	1.78
A 398-1	80	45	134	2.27
A 399-1	120	47	133	2.67
A 400-1	240	47	138	3.38
A 402-1	900	48	99	4.28

Temperature 1190°C

Core No.	Time (Min.)	μ_1 at 2 mc.	Q at 2 mc.	% Fe^{++}
A 375-1	3	98	98	.82
A 376-1	5	37	108	1.30
A 377-2	10	43	113	1.88
A 378-1	15	45	121	2.24
A 379-1	20	48	121	2.43
A 380-1	40	--	---	2.60
A 381-1	80	51	136	3.23
A 382-1	120	52	139	3.65
A 385-1	240	52	125	4.43
A 390-1	630	53	102	5.04
A 389-1	900	53	83	4.97

Temperature 1210°C

Core No.	Time (Min.)	μ_1 at 2 mc.	Q at 2 mc.	% Fe^{++}
A 404-1	3	31	100	1.05
A 405-1	5	42	108	1.48
A 406-1	7	44	108	2.15
A 407-2	10	47	113	2.21
A 408-2	15	50	120	2.72
A 410-1	30	53	119	3.36
A 411-1	40	54	123	3.10
A 412-1	80	55	106	4.06
A 413-1	120	54	120	----
A 415-1	240	56	76	5.02
A 417-1	900	59	69	5.84

Temperature 1230°C

Core No.	Time (Min.)	μ_1 at 2 mc.	Q at 2 mc.	% Fe^{++}
A 418-2	3	40	102	1.68
A 419-1	4	47	98	----
A 420-2	5	56	93	2.6
A 421-1	7	63	97	3.36
A 422-2	10	71	86	3.44
A 433-1	12	71	77	3.83
A 423-1	15	74	99	4.33
A 424-1	20	83	45	5.10
A 426-1	30	83	51	5.01
A 427-1	40	85	56	5.20
A 428-1	60	86	45	5.76
A 429-1	80	93	32	6.06
A 430	120	93	41	6.44
A 432	900	75	50	6.79

TABLE (11)

Curie Temperature for Five Compositions Fired at 1210°C

Composition	T_c
$Ni_{.474}Zn_{.526}Fe_2O_4$	260
$Ni_{.474}Zn_{.526}Fe_2O_4 + .135\ Fe_2O_3$	301
$Ni_{.474}Zn_{.526}Fe_2O_4 + .294\ Fe_2O_3$	351
$Ni_{.474}Zn_{.526}Fe_2O_4 + .570\ Fe_2O_3$	423
$Ni_{.474}Zn_{.526}Fe_2O_4 + .938\ Fe_2O_3$	432

TABLE (12)

Curie Temperature for Material Fired for Various Times at 1210°C

Firing Time (Min.)	Comp. 5 TC	Comp. 5
3	266	432
5	270	450
10	272	456
20	277	456
40	267	432
80	266	430
120	256	428
180	254	436
240	258	430
900	246	---

ACKNOWLEDGMENTS

The authors wish to thank Professor H. W. Welch, Jr., for his continuing encouragement, Mr. Paul E. Nace for standardizing the magnetic measurements and for overseeing much of the detailed work, Mr. Hsien Wu Chang for his many ferrous iron determinations, and finally, both past and present members of Task 6 for numerous smaller contributions.

BIBLIOGRAPHY

20. L. I. Rabkin, "Magnetic Ferrites in Alternating Fields," Bulletin of the Academy of Sciences of the USSR, Physical Series (English translation, Columbia Technical Translations) Vol. 18, 1954.

21. Okamura, Simorzaka and Torizuka, "On the Formation of Semiconductors of the Spinel Type," Science Reports Research Institute, Tohoku University, Series A, 1, 1949.

22. Milligan and Holmes, "X-Ray Diffraction Studies in the System CuO-Fe_2O_3," J. Amer. Chem. Soc., 63, 149-150, 1949.

23. L. M. Watt and W. O. Milligan, "X-Ray Diffraction Studies in the System BeO-In_2O_3," J. Phys. Chem., 57, 883-884, 1953.

24. W. O. Milligan, "Recent X-Ray Diffraction Studies on the Hydrous Oxides and Hydroxides," J. Phys. and Colloid Chem., 55, 497, 1951.

25. R. P. Seelig, "Fundamentals of Pressing of Metal Powders," The Physics of Powder Metallurgy, McGraw-Hill Book Co., Inc., 1951.

26. F. G. Brockman, "The Cation Distribution in Ferrites with Spinel Structure," Phys. Rev., 77, 841-843, 1950.

27. Yogoro Kato and Takeshi Takei, "Studies on Zinc Ferrite: Its Formation, Composition and Chemical and Magnetic Properties," Trans. Amer. Electrochemical Soc., 57, 297-312, 1930.

28. S. V. Berger, "Röntgenundersökningar Av Spinellfasen I Systemet ZnO-Fe_2O_3," Festskrift Tillagnad J. Arvid Hedvall, pp. 31-42, Goteborg, 1948.

29. Isao Kushima and Tsuyoshi Amanuma, "On the Constitution of Zinc Ferrite," Memoirs of the Faculty of Engineering, Kyoto University, 16, 191-203, 1954.

DISTRIBUTION LIST

1 Copy	Director, Electronic Research Laboratory Stanford University Stanford, California Attn: Dean Fred Terman
1 Copy	Commanding General Army Electronic Proving Ground Fort Huachuca, Arizona Attn: Director, Electronic Warfare Department
1 Copy	Chief, Research and Development Division Department of the Army Washington 25, D. C. Attn: SIGEB
1 Copy	Chief, Plans and Operations Division Office of the Chief Signal Officer Washington 25, D. C. Attn: SIGEW
1 Copy	Countermeasures Laboratory Gilfillan Brothers, Inc. 1815 Venice Blvd. Los Angeles 6, California
1 Copy	Commanding Officer White Sands Signal Corps Agency White Sands Proving Ground Las Cruces, New Mexico Attn: SIGWS-CM
1 Copy	Commanding Officer Signal Corps Electronics Research Unit 9560th TSU Mountain View, California
1 Copy	Mr. Peter H. Haas Mine Fuze Division Diamond Ordnance Fuze Laboratories Washington 25, D. C.
1 Copy	Dr. J. K. Galt Bell Telephone Laboratories, Inc. Murray Hill, New Jersey
1 Copy	Dr. R. M. Bozorth Bell Telephone Laboratories, Inc. Murray Hill, New Jersey

1 Copy	Dr. G. T. Rado Naval Research Laboratory Washington 25, D. C.
60 Copies	Transportation Officer, SCEL Evans Signal Laboratory Building No. 42, Belmar, New Jersey FOR - SCEL Accountable Officer Inspect at Destination File No. 22824-PH-54-91(1701)
1 Copy	H. W. Welch, Jr. Engineering Research Institute University of Michigan Ann Arbor, Michigan
1 Copy	J. A. Boyd Engineering Research Institute University of Michigan Ann Arbor, Michigan
1 Copy	Document Room Willow Run Research Center University of Michigan Willow Run, Michigan
11 Copies	Electronic Defense Group Project File University of Michigan Ann Arbor, Michigan
1 Copy	Engineering Research Institute Project File University of Michigan Ann Arbor, Michigan